Ground-state energetics of helium and deuterium fermion fluids

E. Krotscheck* and R. A. Smith†
Department of Physics, State University of New York, Stony Brook, New York, 11794

J. W. Clark and R. M. Panoff
McDonnell Center for the Space Sciences and Department of Physics, Washington University, St. Louis, Missouri 63130
(Received 14 April 1981)

The method of correlated basis functions (CBF) is applied to the evaluation of the ground-state energy of atomic fermion fluids as a function of density. As a first step, liquid ^{3}He in both unpolarized and fully polarized spin configurations is considered variationally, using Slater-Jastrow trial wave functions. Results are reported for a conventional analytic choice of the state-independent two-body correlation function $f(r)$ and for the optimal $f(r)$ determined by the solution of a suitable Euler equation. The Jastrow treatment is found to be inadequate in that (i) the energy expectation value lies above the experimental equilibrium energy by some 1.5 K, and (ii) the polarized phase is predicted to be more stable than the unpolarized one. For a given polarization, a correlated basis is formed by application of the assumed Jastrow correlation factor to the elements of a complete set of noninteracting-Fermi-gas Slater determinants. The exact ground-state energy may be developed in a perturbation expansion in the correlated basis, the leading term being the Jastrow energy expectation value. Considerable improvement on the Jastrow description of the unpolarized phase is achieved upon inclusion of the correlated two-particle–two-hole component of the second-order CBF perturbation correction. At the experimental equilibrium density, this contribution, which incorporates important momentum- and spin-dependent correlations, can amount to some 0.6–1.1 K [depending on the choice of $f(r)$]. The required correlated-basis matrix elements are calculated by Fermi hypernetted-chain (FHNC) techniques, crucial Pauli effects of the elementary diagrams being introduced through the FHNC/C algorithm. The Euler equation is approximated within the same framework. The momentum-space integrations in the second-order perturbation correction are evaluated by a Monte Carlo procedure. One may reasonably expect that further refinements of the CBF method will lead to an accurate microscopic description of the ground-state energetics of liquid ^{3}He. Bulk atomic deuterium with all electronic spins aligned is treated at the same level of approximation as applied to helium. Three choices of nuclear-spin distribution are examined, with a single spin state present, or two or three equally populated nuclear spin states. The finite-density energy minimum is found to lie very close to zero energy in all three examples; a very precise many-body calculation will thus be needed to decide their liquid or gaseous nature at zero temperature under zero external pressure.

I. INTRODUCTION

The expectation that diverse phenomena of fundamental interest will be observable in spin-polarized quantum fluids, stabilized for example by a strong magnetic field at low temperature, is generating a great deal of excitement.[1] In a recent paper by three of us[2] (CKP), a comprehensive microscopic approach to strongly-interacting Fermi fluids was formulated within the method of correlated basis functions, and results were reported for unpolarized and fully polarized ^{3}He and for two species of electron-spin-aligned D. The present article is devoted to important refinements and extensions of that work.

It is convenient for us to adopt the following notation[3] in discussing polarized versions of bulk ^{3}He and deuterium. ^{3}He with all nuclear spins aligned parallel to a reference direction (ordinarily the direction of the magnetic field), will be designated ^{3}He↑, while the unpolarized system may be denoted simply ^{3}He, without an arrow. Deuterium with all electronic spins aligned antiparallel to the field will be symbolized by D↓. The nucleus of the D atom has spin 1 and therefore three possible orientations with respect to the reference direction, $M_S = 0, -1$, and 1. We identify certain especially simple choices of the populations of nuclear spin states in bulk D, labeled D$\downarrow_1$, D$\downarrow_2$, and D$\downarrow_3$. The simplest, D$\downarrow_1$, is a D↓ system in which only one nuclear spin state is occupied (say $M_S = 1$); in D$\downarrow_2$ two nuclear spin states are present (say $M_S = 1, 0$) with equal populations; and D$\downarrow_3$ involves all three nuclear spin states, assumed to be equally occupied. Our calculations are limited to the pure examples ^{3}He↑, ^{3}He, D$\downarrow_1$, D$\downarrow_2$, and D$\downarrow_3$, cases

of partial polarization interpolating these choices being left for future study. In terms of the single-particle level degeneracy ν entering the connection $\rho=\nu k_F^3/6\pi^2$ between density ρ and Fermi wave number k_F, the examples selected correspond, respectively, to $\nu=1$, 2, 1, 2, and 3.

Interest in these systems springs primarily from their extreme quantum nature. Following Nosanow, Parish, and Pinski,[4] one may define a quantum parameter $\eta\equiv\hbar^2/m\epsilon\sigma^2$ in terms of the particle mass m and the depth and range parameters ϵ and σ of a Lennard-Jones fit

$$v(r)=4\epsilon[(\sigma/r)^{12}-(\sigma/r)^6]$$

to the interatomic potential. The larger η, the more important are the effects of quantum zero-point motion.[5] The values $\eta=0.274$ for D$\downarrow$ and $\eta=0.241$ for ^{3}He$\uparrow$ and ^{3}He may be compared to the values $\eta=0.182$, 0.076, and 0.038 for ^{4}He, H_2, and D_2, respectively.

The quantum nature of systems is of course reflected in the effects of statistics as well as zero-point motion. The parameter determining the statistical properties of the systems under study is the degeneracy ν. A given value of ν may be regarded as characterizing either (a) a one-component system of identical fermions, with equal occupation of ν *distinct* internal states, or (b) a ν-component system containing ν distinct fermion species, in equal numbers. [It may be assumed, to a good approximation, that the interaction $v(ij)$ depends only on the separation $r_{ij}=|\vec{r}_i-\vec{r}_j|$, so that any internal, nonclassical degrees of freedom are manifested *only* through ν.] We are presented with the opportunity of studying the behavior of fermion fluids as a function of the degeneracy parameter ν, with all other variables (particle mass, interaction) held fixed. The smaller ν, the more extreme will be the Fermi nature of the system, while $\nu\rightarrow\infty$ with ρ a constant represents the Bose limit.

In this paper we shall concentrate on the ground-state energetics of the designated systems. However, we will not be concerned with subtle effects of the hyperfine interaction (which in the deuterium case would mix in small components of the "wrong" electron-spin state, $\uparrow$). Nor will we include the energy of interaction of the system with any external magnetic fields which may be imposed to maintain the specified polarization.

Our approach to the calculation of the ground-state energy as a function of density (which determines the zero-temperature equation of state) has been described at some length in Ref. 2. The reader may find it necessary to consult that paper for certain details of definition and notation. The essentials of the method of correlated basis functions (CBF) are the following. We adopt a basis of correlated states

$$|\Psi_m\rangle=F|\Phi_m\rangle/\langle\Phi_m|F^\dagger F|\Phi_m\rangle^{1/2}\ , \tag{1}$$

the Φ_m forming a complete orthonormal set of Fermi-gas energy eigenfunctions corresponding to density ρ and degeneracy ν, with $m=0$ denoting the filled Fermi sea. The correlation operator F is taken in state-independent Jastrow form,[6]

$$F=\prod_{i<j}f(r_{ij})=F^\dagger\ , \tag{2}$$

with $f(r)$ either (a) an analytic one-parameter function $f(r)=\exp[-\frac{1}{2}(b/r)^5]$ as employed by Schiff and Verlet[7] (SV), (b) a Pandharipande-Bethe[8] (PB) function, i.e., the lowest solution of a two-body Schrödinger-like equation with outer boundary condition of smooth healing of f to unity at a specified healing distance d, or (c) an "optimal" correlation function, determined by an (approximate) Euler equation derived from the Jastrow energy functional $E[f]\equiv\langle H\rangle=\langle\Psi_0|H|\Psi_0\rangle=H_{00}$. [In cases (a) and (b), the parameters b and d, respectively, may be adjusted so as to minimize $\langle H\rangle$.]

For prescribed f, the ground-state energy is evaluated by nonorthogonal perturbation theory in the Jastrow-correlated basis. The *exact* ground-state energy may be expanded as

$$\mathcal{E}=H_{00}+\delta\mathcal{E}^{(2)}+\delta\mathcal{E}^{(3)}+\cdots+\delta\mathcal{E}^{(n)}+\cdots\ . \tag{3}$$

Formulas for the lowest few CBF perturbation corrections $\delta\mathcal{E}^{(n)}, n=2,3,4$, are given in Ref. 9, in terms of the CBF matrix elements $H_{mn}=\langle\Psi_m|H|\Psi_n\rangle$ and $N_{mn}=\langle\Psi_m|\Psi_n\rangle$. Herein we shall take account of (at most) the leading correction of the Jastrow energy H_{00}, namely the second-order term

$$\delta\mathcal{E}^{(2)}=-\sum_{m\neq0}\frac{|H_{m0}-H_{00}N_{m0}|^2}{H_{mm}-H_{00}}\ . \tag{4}$$

This contribution is itself approximated: we include only the effects of "correlated two-particle–two-hole ($2p$-$2h$) excitations," the sum over m being so restricted that Φ_m differs from the Fermi-gas ground state Φ_0 in exactly two orbitals. The resulting estimate of the energy shift due to non-Jastrow correlations is denoted $\delta\mathcal{E}^{(2,2)}$.

The required CBF matrix elements [or rather, the appropriate combinations H_{00}, $H_{mm}-H_{00}$, and $(H_{mn}-H_{00}N_{mn})(1-\delta_{mn})$ of them] are calculated via the extended Fermi hypernetted-chain (FHNC) procedure outlined in Ref. 2, i.e., in terms of the solutions of the so-called FHNC/C and (FHNC/C)′ equations.

It was found in Ref. 2 that the Jastrow model, based on the *single* correlated configuration $\prod f(r_{ij})\Phi_0$, does not provide an adequate (quantitative) description of the ground state of unpolarized ^{3}He, even if $f(r)$ is determined optimally. We note in particular that (i) momentum-dependent correlations (which, for example, correspond physically to backflow around a moving particle), (ii) spin-

dependent correlations involving the operators $\vec{\sigma}_i \cdot \vec{\sigma}_j$ (and corresponding in particular to spin-density fluctuations), and (iii) direct three-particle correlations [triplet i-j-k correlations not expressible in the form $f(r_{ij})f(r_{ik})f(r_{jk})$] are missing from the Jastrow ansatz. Correlations of types (i) and (iii) have been considered to be the most important for the gross energetics of the system[10]; however, spin-dependent correlations may also have a substantial effect on the energy, and are known to play a crucial role in some system properties such as magnetic susceptibility and superfluidity.[20,31]

It may further be concluded from the results of Ref. 2 that the Jastrow model gives a considerably better description in the case of polarized ^{3}He than it does for the unpolarized system, in the sense that it produces a closer bound on the relevant ground-state energy. This finding is understandable in qualitative terms: in the polarized phase the Pauli principle is more effective in preventing close approach of particles, which reduces the influence of direct three-body correlations (and possibly also of momentum-dependent correlations); moreover, the particles are constrained to interact exclusively in the spin state $|SM_S\rangle = |11\rangle$, which suppresses the role of spin-density fluctuations. Thus the shortcomings of the Jastrow ansatz will be of relatively little consequence in this case, at least if we confine our attention to the ground-state energy.

These conclusions and judgments regarding ^{3}He are generally supported by the Monte Carlo calculations of Levesque[11] based on the Jastrow model (see also Ref. 30). Accordingly, we seek to improve upon the Jastrow variational energy for the unpolarized system by incorporating the CBF correction $\delta\mathcal{E}^{(2,2)}$. Calculation of this correction for the polarized system is precluded by the technical obstacle[2] that singularities arise within the present formulation when ν is reduced from 2 to 1. However, as argued above, it does not appear to be so imperative to go beyond the Jastrow description for ^{3}He$\uparrow$.

The deuterium systems are treated analogously; that is, we adhere to the Jastrow model in the case of $D\downarrow_1$ ($\nu=1$), but include the CBF correction $\delta\mathcal{E}^{(2,2)}$ in the cases $D\downarrow_2$ ($\nu=2$) and $D\downarrow_3$ ($\nu=3$).

In Sec. II we take up certain crucial aspects of the calculational procedure employed, aspects which either were not made explicit in Ref. 2 (CKP) or else reflect significant improvements upon the techniques used in that study. For completeness, the FHNC′ equations are written out explicitly in Appendix A, and some details of the f-optimization routine are described in Appendix B. The Monte Carlo procedure used to compute $\delta\mathcal{E}^{(2,2)}$ is sketched in Appendix C. The current numerical results on the helium and deuterium systems are presented and discussed in Sec. III. Relative to CKP, the main improvement is in the evaluation of $\delta\mathcal{E}^{(2,2)}$, which may now be regarded as quantitatively reliable. Extensions relative to CKP consist of application of the method to $D\downarrow_3$ and calculations on the $D\downarrow$ systems with Pandharipande-Bethe and optimal (as well as Schiff-Verlet) correlation functions.

II. CALCULATION MATTERS

A. Optimization procedures

The variational problem

$$\frac{\delta H_{00}[f]}{\delta \ln f} = 0 \tag{5}$$

is expressed most conveniently in Fourier space, where it reads[12–14,16]

$$(\hbar^2 k^2/4m)[S(k)-1] + S'(k) \equiv \tilde{\omega}(k) = 0 \ . \tag{6}$$

In Eq. (6), $S(k)$ is the static structure function generated by the Jastrow trial state $\Psi_0 = \prod f(r_{ij})\Phi_0$ and $S'(k)$ is a corresponding generalized structure function.[12,14,16] The structure functions $S(k)$ and $S'(k)$ are in turn simply expressible in terms of the compound-diagrammatic quantities of FHNC and FHNC′ theory. An outline of the derivation of the Euler equation (6) and of FHNC equations for $S'(k)$—the so-called FHNC′ equations—is provided in Appendix A.

Three different procedures for solving Eq. (5) are in current use. "Solution" consists here of executing an iterative scheme in one of the key ingredients of variational theory {namely, the correlation function $f(r)$, the radial distribution function $g(r)$, or the FHNC quantity[6] $\Gamma_{dd}(r) \equiv f^2(r)\exp[N_{dd}(r)+E_{dd}(r)] - 1$} until convergence of $\tilde{\omega}(k)$ to zero is achieved. The three procedures are (i) the Lagrange-multiplier technique of Lantto and Siemens,[15] aimed at determining the optimal $g^{1/2}(r)$, (ii) Owen's simplified Newton-Raphson iterative scheme[13] for producing the optimal $\Gamma_{dd}(r)$ {or rather $g_B^{1/2}(r) = [1+\Gamma_{dd}(r)]^{1/2}$}, and (iii) straightforward adaptation of the working formulas of the paired-phonon analysis[16] (PPA) to yield a solution essentially for the optimal $f(r)$.

Taking the Lantto-Siemens approach, one works in practice with Euler-Lagrange equations based on functional variation of an *approximate* expression for the energy functional $H_{00}[f]$ (in particular, the FHNC/0 approximation,[2,6] being used). On the other hand, in methods (ii) and (iii), one approximates the Euler equation derived from the *exact* $H_{00}[f]$ (the FHNC/C versions[2,17] of various compound diagrammatic quantities being inserted); after solving this approximate equation the energy expectation value is computed via a correspondingly approximate energy functional. The latter strategy has the advantage that certain exact properties of the compound-

diagrammatic ingredients of the theory (see Appendix A) may be preserved; it is then possible to establish unambiguously that the structure function $S(k)$ associated with the Jastrow state has the proper long-wavelength behavior. A (usually minor) disadvantage of procedures (ii) and (iii) is that, in some cases, the value obtained for the approximate energy functional at the resulting optimal f is found to lie slightly higher than for a suitably chosen Schiff-Verlet function f_{SV}. This can happen because f_{opt} is *not* determined by minimizing the approximate functional with respect to f.

Application of the Lantto-Siemens Lagrange-multiplier technique in conjunction with the FHNC/0 approximation is precluded here by the following consideration. As explained in Sec. II B, the compound-diagrammatic products or by-products of optimal FHNC theory enter into the subsequent evaluation of CBF quantities and especially the CBF perturbation correction. The Lantto-Siemens FHNC/0 prescription leads, unfortunately, to an unacceptable large-r behavior for the effective perturbation. [In the language of FHNC′ theory,[2] one finds[15] $\Gamma'_{dd}(r) \sim r^{-2}$ $(r \to \infty)$.] Accordingly, our numerical investigations have been confined to the Newton-Raphson treatment (ii) and paired-phonon analysis (iii). We hasten to add that the procedure of Ref. 15 will be equivalent to (ii) and (iii) as applied below, provided the same low-k corrections—viz., those of the FHNC/C scheme—are made.

In Owen's procedure (ii), the Euler equation is linearized, i.e.,

$$\omega(r) + \int d\vec{r}' \left(\frac{\delta\omega(r)}{\delta g_B^{1/2}(r')} \right) \delta g_B^{1/2}(r') = 0 \tag{7}$$

is used to generate a correction $\delta g_B^{1/2}(r)$ to a given iterate $g_B^{1/2}(r)$ [at which $\omega(r) \equiv (2\pi)^{-3}\rho^{-1} \int \tilde{\omega}(k) \times \exp(i\vec{k}\cdot\vec{r})\, d\vec{k}$ and the derivative in large parentheses is evaluated]. If we exploit the fact that the derivative need only be roughly correct, this equation can be simplified considerably; thus

$$-\tilde{\omega}(k)/S_F(k) = -(\hbar^2 k^2/m)[\delta g_B^{1/2}(r)]^{\mathfrak{F}}(k) + S_F(k)[v(r)\delta g_B^{1/2}(r)]^{\mathfrak{F}}(k) \tag{8}$$

suffices for the determination of $\delta g_B^{1/2}(r)$. In the latter equation, the $\mathfrak{F}$ superscript stands for dimensionless Fourier transform, e.g., $X^{\mathfrak{F}}(k) = \rho \int X(r) \exp(i\vec{k}\cdot\vec{r})\, d\vec{r}$, and $S_F(k)$ is the structure function of the noninteracting Fermi gas. For further details, see Ref. 13.

Turning to the PPA scheme, a correction $\delta u(r)$ to a given iterate for $u(r) = \ln f^2(r)$ is formed (in Fourier space) via

$$\delta\tilde{u}(k) = S^{-1}(k)\{1 - [S(k) + (4m/\hbar^2 k^2)S'(k)]^{1/2}\} , \tag{9}$$

where $S(k)$ and $S'(k)$ are computed with $u(r)$. A corresponding correction $\delta\Gamma_{dd}(r)$ to the latest $\Gamma_{dd}(r)$ is obtained by linearizing the FHNC equation for $\Gamma_{dd}(r)$ and making use of Eq. (9),

$$\begin{aligned} &\delta\Gamma_{dd}(r) = [1 + \Gamma_{dd}(r)][\delta u(r) + \delta N_{dd}(r)] , \\ &\delta\tilde{u}(k) + \delta\tilde{N}_{dd}(k) = S_d^2(k)\{1 - [S(k) + (4m/\hbar^2 k^2)S'(k)]^{1/2}\} S^{-1}(k) , \end{aligned} \tag{10}$$

where we have reverted to the conventional tilde notation for dimensionless Fourier transform and Γ_{dd}, N_{dd}, and S_d are as defined in CKP (Ref. 2) or Appendix A.

It is found that these two iteration methods, Newton-Raphson and paired phonon, are comparably efficient, the latter having the small advantage that numerical second differentiation can be avoided at sensitive places. Some technical features of the numerical procedures we have adopted are taken up in Appendix B. However, we should mention here that both Newton-Raphson and paired-phonon iteration schemes rely on fulfillment of the exact long-wavelength properties $S(k) \sim k$ and $S'(k) \sim k^2 (k \to 0+)$. Indeed, within the context of the FHNC/0 approximation (which does not maintain these properties) the two schemes are not applicable, unless a very special iteration path is followed whose consistency with the proper low-momentum behavior of $S(k)$ and $S'(k)$ is yet to be established. Therefore we are led quite naturally to the use, in the optimization problem, of the FHNC/C approximation of Ref. 17 (or the successive approximations of the Krotscheck-Ristig version of FHNC theory[6,13,18]) for the required compound-diagrammatic quantities. These approximations involve simple estimates of the crucial elementary diagrams so as to preserve the aforesaid long-wavelength properties of $S(k)$ and $S'(k)$. Consequently they guarantee, at the level of a transparent and rigorous identity, the correct large-r asymptotic behavior $f(r) - 1 \sim r^{-2}$ of the optimal correlation function—provided only that a stable solution of the variational problem exists. By contrast, in the current Lantto-Siemens scheme the correct asymptotic behavior must result from certain delicate nontrivial cancellations.

B. Single-particle energies and effective interactions

It is an especially attractive feature of the formulation of the optimization problem in terms of the FHNC and FHNC′ equations, that its execution

yields as natural by-products the essential ingredients of further attributes of the Jastrow model such as single-particle energies (and effective mass), magnetic susceptibility, and pairing matrix elements.[2,19,20] But in addition, these same by-products furnish the raw material for an improvement upon the Jastrow description via the method of correlated basis functions. To be more explicit: two of us[19] have recently extended the conventional diagrammatic cluster-expansion resummation techniques to nondiagonal matrix elements in the Jastrow-correlated basis (1)-(2), and have shown how to construct effective interactions as well as single-particle energies in terms of quantities generated automatically upon solution of the FHNC and FHNC′ equations. In this work, the Clark-Westhaus (CW) prescription[6,9] for expressing matrix elements of the kinetic-energy operator was employed. On the other hand, the optimization procedures sketched above are tied to the Jackson-Feenberg (JF) form[6,12] for $\langle H\rangle$. Accordingly, we have reformulated the construction of Ref. 19 in terms of the JF treatment of the kinetic energy which, though somewhat more complicated than that of CW, has the distinctive virtue that the three-body terms it produces are almost negligible. The required formulas are derived from the Jackson-Feenberg operator identity

$$F\nabla^2 F=\tfrac{1}{2}(\nabla^2F^2+F^2\nabla^2)+\tfrac{1}{2}F^2[\nabla,[\nabla,\ln F]]-\tfrac{1}{4}[\nabla,[\nabla,F^2]] \ , \quad (11)$$

sandwiched between model states $\langle\Phi_m|$ on the left and $|\Phi_n\rangle$ on the right.

Consider now the assembly of $\delta\mathcal{S}^{(2,2)}$ using expression (4), with the sum restricted to correlated two-particle–two-hole ($2p$-$2h$) excitations, corresponding to $|\Phi_m\rangle$ of the type $a^\dagger_{p_1}a^\dagger_{p_2}a_{h_2}a_{h_1}|\Phi_0\rangle$. The energy denominator of Eq. (4) is then given by

$$H_{mm}-H_{00}=e(p_1)+e(p_2)-e(h_1)-e(h_2) \ , \quad (12)$$

i.e., as the difference of the Jastrow single-particle energies[19] of particles and holes,

$$e(\lambda)=t(\lambda)+u(\lambda)+U_0 \quad (13)$$

($\lambda=p_1,p_2,h_1,h_2$). In the latter expression, $t(\lambda)\equiv\hbar^2k_\lambda^2/2m$, U_0 is an irrelevant addend independent of momentum, and the nontrivial quantity

$$u(\lambda)=\frac{\tilde X'_{cc}(k_\lambda)}{1-\tilde X_{cc}(k_\lambda)}+\frac{\hbar^2k_\lambda^2}{2m}[\tfrac{1}{2}\tilde X_{cc}(k_\lambda)+Y(k_\lambda)] \ , \quad (14)$$

with

$$i\vec k_\lambda Y(k_\lambda)=[\nabla_1^{(l)}X_{cc}(r_{12})]^{\mathfrak{F}}(k_\lambda)-i\vec k_\lambda\tilde X_{cc}(k_\lambda) \ , \quad (15)$$

represents the average momentum-dependent field. The compound-diagrammatic inputs $\tilde X_{cc}(k_\lambda)$ and $\tilde X'_{cc}(k_\lambda)$ have been specified in Ref. 2 (see also Appendix A), and $l(k_Fr)$ is the familiar Slater exchange-line function, $l(x)=3x^{-3}(\sin x-x\cos x)$. The gradient $\nabla_1^{(l)}$ in Eq. (15) is supposed to act only on the exchange line attached to point 1.

The combination $H_{m0}-H_{00}N_{m0}$ of off-diagonal CBF matrix elements entering the numerator of the $2p$-$2h$ summand in Eq. (4) serves to define a nonlocal two-body effective perturbation operator $\mathfrak{V}(12)$. Calling on results from Ref. 19 (cf. also Ref. 20), we may write

$$\begin{aligned}H_{m0}-H_{00}N_{m0}&\equiv\langle p_1p_2|\mathfrak{V}(12)|h_1h_2\rangle_a\\&=\langle p_1p_2|\mathfrak{W}(12)|h_1h_2\rangle_a\\&\quad+\tfrac{1}{2}[e(p_1)+e(p_2)-e(h_1)-e(h_2)]\\&\quad\times\langle p_1p_2|\mathfrak{N}(12)|h_1h_2\rangle_a \ ,\end{aligned} \quad (16)$$

wherein the two-body matrix elements of the nonlocal operators $\mathfrak{N}(12)$ and $\mathfrak{W}(12)$ have the factorizable structure

$$\langle p_1p_2|\mathfrak{N}(12)|h_1h_2\rangle_a=D^{-1}\langle p_1p_2|\mathfrak{N}^B(12)|h_1h_2\rangle_a \ , \quad (17)$$

$$\langle p_1p_2|\mathfrak{W}(12)|h_1h_2\rangle_a=D^{-1}[\langle p_1p_2|\mathfrak{W}^B(12)|h_1h_2\rangle_a+\tfrac{1}{2}[u(p_1)+u(p_2)+u(h_1)+u(h_2)]\langle p_1p_2|\mathfrak{N}^B(12)|h_1h_2\rangle_a] \ ,$$

with

$$D\equiv\{[1-\tilde X_{cc}(k_{p_1})][1-\tilde X_{cc}(k_{p_2})][1-\tilde X_{cc}(k_{h_1})][1-\tilde X_{cc}(k_{h_2})]\}^{1/2} \quad (18)$$

The subscript "a" means antisymmetrized. The reduced nonlocal operators $\mathfrak{N}^B(12)$ and $\mathfrak{W}^B(12)$ are given by expansions in basic diagrams as defined in Ref. 19.

The simplest approximations to $\mathfrak{N}^B(12)$ and $\mathfrak{W}^B(12)$ consist in retaining the leading terms of their respective diagrammatic expansions, these leading terms being local. More explicitly, one adopts

$$\mathfrak{N}^B(12)\approx\mathfrak{N}^B_{\rm loc}(12)=\Gamma_{dd}(r_{12}) \ ,$$
$$\mathfrak{W}^B(12)\approx\mathfrak{W}^B_{\rm loc}(12)=\Gamma'_{dd}(r_{12})+(\hbar^2/4m)\nabla^2\Gamma_{dd}(r_{12}) \ , \quad (19)$$

with $\Gamma_{dd}(r_{12})$ and $\Gamma'_{dd}(r_{12})$ as specified in Appendix

A [the prime denoting the graphical derivative of $\Gamma_{dd}(r_{12})$, *not* its gradient].

It must be pointed out, however, that the local approximation to $\mathfrak{N}^B(12)$ gives, for long-range correlations $f(r)-1=O(r^{-2})$, $r\to\infty$, the *wrong* strength for the singularity of $\langle p_1p_2|\mathfrak{N}(12)|h_1h_2\rangle$ occurring at zero momentum transfer, i.e., in the limit $\hbar|\vec{k}_{p_1}-\vec{k}_{h_1}|\equiv\hbar q\to 0$. This defect is ascribable to the neglect of "elementary" diagrams, the archetypical set of which is shown in Fig. 1. The sum of contributions from all diagrams of the indicated topological structure, taken together with the leading, local contribution, may be cast in the form

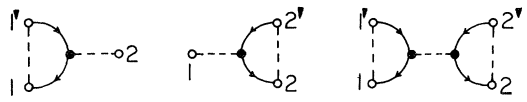

FIG. 1. Elementary diagrams contributing to the nonlocal operator $\mathfrak{N}^B(12)$, whose kernel in configuration space is denoted $\mathfrak{N}^B(12;1'2')$ (see Ref. 19).

$$\langle p_1p_2|\mathfrak{N}^B(12)|h_1h_2\rangle=[1+\tilde{E}_{ecc}(p_1,h_1)][1+\tilde{E}_{ecc}(p_2,h_2)]\langle p_1p_2|\Gamma_{dd}(r_{12})|h_1h_2\rangle\ , \tag{20}$$

with $\tilde{E}_{ecc}(p,h)\to-\tilde{X}_{cc}(k_F)$ in the $q\to 0$ limit. Corresponding "elementary-diagram" contributions to $\mathbf{W}^B(12)$ are generated from $D^{-1}\langle p_1p_2|\mathfrak{N}^B(12)|h_1h_2\rangle$ by graphical differentiation. We arrive at the representation

$$\begin{aligned}D\langle p_1p_2|\mathbf{W}(12)|h_1h_2\rangle=&[1+\tilde{E}_{ecc}(p_1,h_1)][1+\tilde{E}_{ecc}(p_2,h_2)]\langle p_1p_2|\mathbf{W}^B_{\rm loc}(r_{12})|h_1h_2\rangle\\&+(\tfrac{1}{2}[[u(p_1)+u(h_1)][1+\tilde{E}_{ecc}(p_1,h_1)]+2\tilde{E}'_{ecc}(p_1,h_1)][1+\tilde{E}_{ecc}(p_2,h_2)]\\&+\tfrac{1}{2}[[u(p_2)+u(h_2)][1+\tilde{E}_{ecc}(p_2,h_2)]+2\tilde{E}'_{ecc}(p_2,h_2)][1+\tilde{E}_{ecc}(p_1,h_1)])\\&\times\langle p_1p_2|\Gamma_{dd}(r_{12})|h_1h_2\rangle\ ,\end{aligned} \tag{21}$$

which unites the "elementary" contributions to the $\mathbf{W}^B$ matrix element (factorable contributions involving E and/or E' quantities) with the separable terms in u arising from the structural decomposition (17). The property

$$\lim_{q\to 0}\tilde{E}'_{ecc}(p,h)=-u(k_F)[1-\tilde{X}_{cc}(k_F)]$$

guarantees the regularity of $D\mathbf{W}$ and hence $D\mathfrak{V}$ in the limit of zero momentum transfer.

It is to be stressed that when $\Gamma_{dd}(r)$ is of long range [as in the case that $f(r)$ is determined optimally], we must not retain the u terms in Eq. (21) while neglecting their "elementary" (E and/or E') counterparts. Such a procedure would lead to a singular behavior of $H_{m0}-H_{00}N_{m0}$ at the Fermi surface (or more precisely in the $q\to 0$ limit). The cancellation of this singularity by the "elementary" contributions to $\mathbf{W}^B(12)$ has the same physical origin—namely, wave-function antisymmetry—as the cancellations, alluded to in Sec. II A, which are responsible for the correct long-wavelength behavior of the structure functions. In concert with the /C treatment of the FHNC and FHNC′ equations, we estimate the effect of the essential elementary quantities by setting

$$\begin{aligned}&\tilde{E}_{ecc}(p,h)\approx\tfrac{1}{2}[S_F(|\vec{k}_p-\vec{k}_h|)-1][\tilde{X}_{cc}(k_p)+\tilde{X}_{cc}(k_h)]\ ,\\&[u(p)+u(h)][1+\tilde{E}_{ecc}(p,h)]+2\tilde{E}'_{ecc}\approx S_F(|\vec{k}_p-\vec{k}_h|)[u(p)+u(h)]\ .\end{aligned} \tag{22}$$

Again, justification for this sort of estimate derives not only from numerical experience with the relevant elementary diagrams, but also from the fact that in the present case these diagrams have little effect other than to eradicate the singularity at $q\to 0$. Once the singularity is removed, the main contributions to the second-order correction $\delta\mathcal{E}^{(2,2)}$ come from the regime of moderate momentum transfer, $q\lesssim 2k_F$, where the elementary diagrams are practically negligible.

Besides the u and E (and/or E') terms collected in Eq. (21), another set of factorizable contributions to the $\mathbf{W}^B(12)$ matrix elements must be identified, which are generated in the JF treatment of the kinetic energy. Specifically, they arise from manipulations in which one of the ∇_i of the kinetic energy operator acts on one of the exchange-line factors of one of the X_{cc} functions appearing in the normalization denominator D, the other ∇_i acting either on the momentum-transfer exponential or on an exchange-line factor in another X_{cc} function present in D. Following the graphical analysis of Ref. 19, we can express these separable "kinetic" contributions through

$$\langle p_1 p_2|\mathbf{w}^B_{\rm kin}(12)|h_1 h_2\rangle = (\hbar^2/4m)\{-(\vec{k}_{p_1}-\vec{k}_{h_1})\cdot[\vec{k}_{p_1}Y(p_1)-\vec{k}_{p_2}Y(p_2)-\vec{k}_{h_1}Y(h_1)+\vec{k}_{h_2}Y(h_2)]$$
$$+\vec{k}_{p_1}\cdot\vec{k}_{h_1}Y(p_1)Y(h_1)+\vec{k}_{p_2}\cdot\vec{k}_{h_2}Y(p_2)Y(h_2)\}\langle p_1 p_2|\Gamma_{dd}(r_{12})|h_1 h_2\rangle \quad . \tag{23}$$

Finally, there are separable contributions which combine elementary (sub-) diagrams entering Eq. (21) and "kinetic" (sub-) diagrams of Eq. (23); these contributions are generated from Eq. (21) by replacement of the factor

$$\tfrac{1}{2}\{[u(p_i)+u(h_i)][1+\tilde{E}_{ecc}(p_i,h_i)]+2\tilde{E}'_{ecc}(p_i,h_i)\}$$

by

$$(\hbar^2/4m)\{-(\vec{k}_{p_i}-\vec{k}_{h_i})\cdot[\vec{k}_{p_i}Y(p_i)-\vec{k}_{h_i}Y(h_i)]+\vec{k}_{p_i}\cdot\vec{k}_{h_i}Y(p_i)Y(h_i)]\}, \quad i=1,2 \quad .$$

Let us step back momentarily to the local approximation (19) to $\mathfrak{N}^B(12)$ and $\mathbf{w}^B(12)$ and spell out a corresponding "local" approximation to the effective perturbation. We observe that quite generally—i.e., whatever one uses for $\mathfrak{N}^B$ and $\mathbf{w}^B$—the separable numerator terms in the hole quantities $u(h_1)$, $u(h_2)$ may be entirely cancelled off upon substitution of Eqs. (13) and (17) into Eq. (16). On the other hand, the separable numerator terms of Eq. (17) involving the particle u's remain. From the foregoing remarks about singularities it is clear that consistency requires the deletion of these latter terms when the local approximation (19) is invoked.

C. Numerical evaluation of perturbation corrections

We have carried out extensive numerical analysis of the second-order correction, based on (a) an "angle-averaging" method patterned after MacKenzie's treatment[21] of the ordinary second-order perturbation correction for soft potentials and (b) Monte Carlo evaluation of the six-dimensional integral involved in $\delta\mathcal{E}^{(2,2)}$. Procedure (a) has been used in earlier calculations within CBF perturbation theory (for example, Refs. 2, 9, 22, and 23). Essential elements of this procedure are (i) partial-wave expansion of the effective-perturbation matrix elements, (ii) angle averaging of the Pauli operator, (iii) quadratic ("effective-mass") approximation of the field function u for holes, neglect for u for particles, and (iv) averaging of the $1-\tilde{X}_{cc}$ factors in the denominator D of Eq. (17) over the angle between center-of-mass and relative momenta, according to

$$[1-\tilde{X}_{cc}(k_{p_1})][1-\tilde{X}_{cc}(k_{p_2})] \rightarrow \{1-\tilde{X}_{cc}[(k_{p_1}^2+k_{p_2}^2)/2]^{1/2}\}^2$$

(and similarly for hole factors). Procedure (b) is described in Appendix C.

Our studies reveal that—at least for unpolarized ^{3}He—substantial cancellations between central and noncentral portions of $\mathbf{v}(12)$ seriously limit the accuracy of the "angle-averaging" prescription. In particular, consider the weighted average

$$\sum_{h_1 h_2}\left[\frac{I_{mm}}{I_{00}}\right]^{1/2}(H_{m0}-H_{00}N_{m0}) = I_{00}^{-1}\langle\Phi_0|F^\dagger(H-H_{00})F\rho_{\vec{q}}\rho_{-\vec{q}}|\Phi_0\rangle \tag{24}$$

of the CBF perturbation $H_{m0}-H_{00}N_{m0}$, where $|\Phi_m\rangle$ is a $2p$-$2h$ state characterized by momentum transfer $\hbar\vec{q}$, $I_{nn}\equiv\langle\Phi_n|F^\dagger F|\Phi_n\rangle$, and $\rho_{\vec{q}}=\sum_i e^{i\vec{q}\cdot\vec{r}_i}$. It is easily seen that the right-hand side of Eq. (24) coincides with $\tilde{\omega}(q)$ as defined by Eq. (6). Thus the left-hand side of Eq. (24) should vanish identically in q for an optimal Jastrow function. However, in actual calculation this condition will hold only if the Pauli operator associated with the h_1, h_2 sums is treated exactly—which is surely not the case in the MacKenzie procedure (a). More broadly, the consequences of angle averaging, especially for systems in which the bare interaction itself does not introduce any overt state dependence into the problem, are difficult to assess. Uncertainties due to the approximation (iii) for the quantities u further erode the reliability of method (a), though errors due to (i) and (ii) may actually be compensated somewhat by those due to (iii). [Approximation (iv) turns out to be rather accurate, owing to the fact that $\tilde{X}_{cc}(k)$ is a slowly-varying function over the relevant interval.] At any rate, Monte Carlo integration allows us to bypass (i)—(iv) and perform a quantitatively reliable evaluation of the perturbation correction.

Valuable insights into proper numerical evaluation of CBF perturbation corrections have been gained in another recent numerical study.[23] However, that work focused on a simple potential model of nuclear matter (the OMY model[6]), and one need not expect approximation techniques which work well there to be as effective under the more extreme conditions of small particle spacing, strong correlation, and (specifically) strongly energy-dependent effective mass[20] found in helium.

III. RESULTS

A. Helium systems

Our calculations for unpolarized ^{3}He and for ^{3}He↑ are based on the standard Lennard-Jones potential with $\epsilon = 10.22$ K and $\sigma = 2.556$ Å. Results are presented here for Schiff-Verlet and optimal correlation functions, denoted, respectively, by $f_{SV}(r)$ and $f_{opt}(r)$. The range parameter b in f_{SV} was simply fixed at the value $b = 2.888$ Å $= 1.13\sigma$ arrived at in Ref. 7, no attempt being made to redetermine a best b at each degeneracy ν and density ρ within the context of our theory. [Judging from our results for $\langle H \rangle$ using f_{opt}, we expect that only a small lowering of the Jastrow energy would accompany such a redetermination (see also Ref. 11).] The compound-diagrammatic quantities (Γ_{dd}, Γ'_{dd}, X_{cc}, etc.), needed in the computation of the Jastrow energy $\langle H \rangle = H_{00}$, in the construction of the Euler equation $\tilde{\omega}(k) = 0$, and in the calculation of the CBF perturbation correction $\delta\mathcal{E}^{(2,2)}$ were evaluated in the FHNC/C approximation. The iteration procedure (iii) described in Sec. II A (i.e., the PPA procedure) was used to obtain f_{opt}.

Extensive numerical results on the Jastrow ground-state energy $\langle H \rangle$ are collected in Table I (wherein CW, JF, and PB refer, respectively, to the use of Clark-Westhaus, Jackson-Feenberg, and Pandharipande-Bethe forms for the kinetic-energy expectation value[6]). Detailed information on the behavior of the second-order correction $\delta\mathcal{E}^{(2,2)}$ is provided in Tables II and III (an effective interaction in JF form being adopted). As usual, energy entries are given in K per particle.

Commenting on Table I, we should point out that the SV entries differ somewhat from the values given in CKP (Ref. 2) due to improvement of the numerics, particularly with regard to the treatment of large-r effects of the correlations. The f_{opt} entries are also somewhat different, for the same reason. Note that for the unpolarized system we now report some results at ρ values beyond the empirical equilibrium density $\rho_e = 0.0164$ Å^{-3}. The reader should concentrate on the JF values for the energy, as these are known [from formal considerations and also from comparison with the results of Monte Carlo (MC) evaluation[11] of $\langle H \rangle$] to be generally the most reliable. Typically (see for example Ref. 6) the exact Jastrow energy lies somewhere between $\langle H \rangle_{JF}$ and $\langle H \rangle_{PB}$, the estimate $\langle H \rangle_{JF}$ thus providing a safe upper bound. [In the ^{3}He systems, $\langle H \rangle_{MC}$ for f_{SV} is closer to $\langle H \rangle_{JF}$ than to $\langle H \rangle_{PB}$, over the interesting density range (see Fig. 2).]

The changes in numerical methods put into effect here will of course have some repercussions for other properties of the Jastrow model which were extracted in CKP, in particular the effective mass m^* at the Fermi surface, the dimensionless pairing matrix elements δ, and the magnetic susceptibility χ. However, the associated modifications are of minor significance, especially in view of the fact that the Jastrow predictions for the latter properties have been shown to be physically incorrect. Quantitative treatment of m^* (for unpolarized ^{3}He and for ^{3}He↑) and of χ and the various δ (for unpolarized ^{3}He) require further development of the method of correlated basis functions[24] or some other approach transcending the Jastrow model.

One may notice upon close inspection of Table I that, at the higher densities, $\langle H \rangle_{JF}$ ($\nu = 2$) evaluated with $f = f_{opt}$ actually lies slightly *above* $\langle H \rangle_{JF}$ ($\nu = 2$) evaluated with $f = f_{SV}$. The excess reaches some 0.1–0.2 K, a discrepancy that is significant relative to the scale of numerical errors (less than 0.1 K) intrinsic to our computations. This anomaly is a reflection of the fact that we have not treated the Euler equation $\tilde{\omega}(k) = 0$ exactly (the FHNC/C approximation, with its limited accounting of elementary-diagram effects, has been applied) and we have not carried out

TABLE I. Jastrow ground-state energies of unpolarized ^{3}He and of ^{3}He↑. Energies in K per particle.

		^{3}He, f_{SV}			^{3}He↑, f_{SV}			^{3}He, f_{opt}			^{3}He↑, f_{opt}		
ρ (10^{-3} Å^{-3})	$\rho\sigma^3$	$\langle H \rangle_{CW}$	$\langle H \rangle_{JF}$	$\langle H \rangle_{PB}$	$\langle H \rangle_{CW}$	$\langle H \rangle_{JF}$	$\langle H \rangle_{PB}$	$\langle H \rangle_{CW}$	$\langle H \rangle_{JF}$	$\langle H \rangle_{PB}$	$\langle H \rangle_{CW}$	$\langle H \rangle_{JF}$	$\langle H \rangle_{PB}$
7.6	0.127	−0.48	−0.58	−0.71	−0.05	−0.24	−0.48	−0.70	−0.72	−0.76	−0.52	−0.54	−0.58
11.2	0.187	−0.56	−0.93	−1.34	−0.18	−0.84	−1.63	−0.78	−1.00	−1.27	−0.78	−1.07	−1.45
13.0	0.217	−0.38	−0.96	−1.60	−0.06	−1.07	−2.29	−0.58	−0.98	−1.45	−0.77	−1.29	−1.95
14.2	0.237	−0.15	−0.91	−1.75	0.11	−1.16	−2.75	−0.33	−0.91	−1.56	−0.65	−1.34	−2.28
14.8	0.247	0.00	−0.87	−1.81	0.22	−1.21	−2.99	−0.16	−0.84	−1.61	−0.55	−1.36	−2.45
16.6	0.277	0.60	−0.63	−1.95	0.66	−1.33	−3.74	0.52	−0.52	−1.67	−0.09	−1.34	−2.93
18.0	0.301	1.25	−0.31	−2.02	...	...	...	1.26	−0.13	−1.70	...	...	...
20.0	0.334	2.44	0.30	−2.02	...	...	...	2.87	0.66	−1.63	...	...	...

TABLE II. Data on perturbation correction in unpolarized ^{3}He for f_{SV}. Energies in K per particle. The last column is taken as standard and denoted $\delta\mathcal{E}^{(2,2)}$.

ρ (10^{-3} Å^{-3})	$\delta\mathcal{E}_{AA}^{(2,2)}\{\alpha_0\}$	$\delta\mathcal{E}_{MC}^{(2,2)}\{\alpha_0\}$	$\delta\mathcal{E}_{MC}^{(2,2)}\{\alpha\}$	$\delta\mathcal{E}_{MC}^{(2,2)}\{\beta\}$
7.6	$e(h) > e(p)$	$e(h) > e(p)$	−0.46 ±0.02	−0.26 ±0.01
11.2	−0.66	−1.0	−0.83 ±0.04	−0.47 ±0.02
13.0	−0.89	−1.2	−1.07 ±0.04	−0.62 ±0.03
14.2	−1.07	−1.5	−1.27 ±0.05	−0.75 ±0.03
14.8	−1.18	−1.6	−1.38 ±0.05	−0.82 ±0.04
16.6	−1.56	−2.1	−1.77 ±0.06	−1.08 ±0.05
18.0	−1.93	. . .	−2.17 ±0.07	−1.35 ±0.04
20.0	. . .	. . .	−2.85 ±0.07	−1.84 ±0.05

an exact evaluation of $\langle H\rangle$ (again, the FHNC/C approximation has been used). More precisely, one should say that $\tilde{\omega}(k)=0$ and $\langle H\rangle$ have not been treated consistently.[16] Thus, $\epsilon \equiv \langle H\rangle_{JF}[f_{opt}] - \langle H\rangle_{JF}[f_{SV}]$, if positive, provides a measure of the inconsistency of the FHNC/C approximation. That this measure is found to grow with density in unpolarized ^{3}He is in line with the density dependence of elementary-diagram contributions; that $\epsilon(\nu=2)$ is still relatively small near the experimental equilibrium density gives reassurance that our computational techniques are reasonable. It is also noteworthy that no such inconsistency surfaces in our results for the spin-aligned phase—perhaps only because the f_{SV} choice with $b=1.13\sigma$ is not so propitious in this case. More definitive information on the precision of the FHNC/C scheme will be examined toward the end of this subsection.

But now let us consider Tables II and III, which juxtapose the results of a variety of numerical treatments of the second-order CBF correction $\delta\mathcal{E}^{(2,2)}$ in unpolarized ^{3}He. The following notational conventions serve to identify the various approximations. The subscripts on $\delta\mathcal{E}^{(2,2)}$ indicate how the integrations implied by the sum over label m were performed: AA for partial-wave expansion plus angle averaging, MC for Monte Carlo integration. The symbols in curly brackets refer to the specific treatment of single-particle quantities and of nonlocal contributions to $\mathfrak{W}^B$ and $\mathfrak{N}^B$, and the disposition of the $(1-\tilde{X}_{cc})^{1/2}$ factors of D^{-1} [see Eqs. (12)–(23)]. Thus, $\{\alpha_0\}$ involves quadratic approximation of $u=u(h)$ for holes, neglect of $u=u(p)$ for particles, omission of all nonlocal contributions to $\mathfrak{W}^B$ and $\mathfrak{N}^B$, and averaging of D as described in Sec. II C; in approximation $\{\alpha\}$ one continues to drop the $u(p)$ terms in the $\mathfrak{V}$ formulas (16) and (17) and the aforesaid nonlocal contributions, but $u(p)$, $u(h)$, $\tilde{X}_{cc}(p)$, and $\tilde{X}_{cc}(h)$ as given by the FHNC/C evaluation received "exact" numerical treatment in the energy denominator $H_{mm}-H_{00}$ and in D; finally, approximation $\{\beta\}$ improves on $\{\alpha\}$ by including, within the /C framework, the u terms of Eqs. (16) and (17) and indeed *all* the nonlocal separable contributions identified in Section II C. This set of approximations is rooted in the notion of expanding $\mathfrak{W}^B(12)$ and $\mathfrak{N}^B(12)$, as they stand in Eq. (17), in basic-diagram series.[19,20]

TABLE III. Data on perturbation correction in unpolarized ^{3}He for f_{opt}. Energies in K per particle. The β evaluation (fourth column) is taken as standard and denoted $\delta\mathcal{E}^{(2,2)}$.

ρ (10^{-3} Å^{-3})	$\delta\mathcal{E}_{AA}^{(2,2)}\{\alpha_0\}$	$\delta\mathcal{E}_{MC}^{(2,2)}\{\alpha\}$	$\delta\mathcal{E}_{MC}^{(2,2)}\{\beta\}$	$\delta\mathcal{E}_{MC}^{(2,2)}\{\alpha a\}$	$\delta\mathcal{E}_{MC}^{(2,2)}\{\beta a\}$
7.6	. . .	−0.22 ±0.014	−0.21 ±0.005	−0.13 ±0.006	−0.20 ±0.01
11.2	−0.33	−0.40 ±0.02	−0.35 ±0.009	−0.22 ±0.007	−0.30 ±0.02
13.0	−0.45	−0.52 ±0.03	−0.44 ±0.01	−0.28 ±0.008	−0.36 ±0.02
14.2	−0.55	−0.61 ±0.03	−0.51 ±0.01	−0.33 ±0.008	−0.42 ±0.02
14.8	−0.60	−0.66 ±0.03	−0.55 ±0.02	−0.36 ±0.008	−0.45 ±0.02
16.6	−0.78	−0.83 ±0.03	−0.68 ±0.02	−0.46 ±0.01	−0.55 ±0.02
18.0	−0.95	−0.99 ±0.03	−0.81 ±0.02	−0.55 ±0.01	−0.64 ±0.02
20.0	. . .	−1.23 ±0.03	−1.04 ±0.03	. . .	. . .

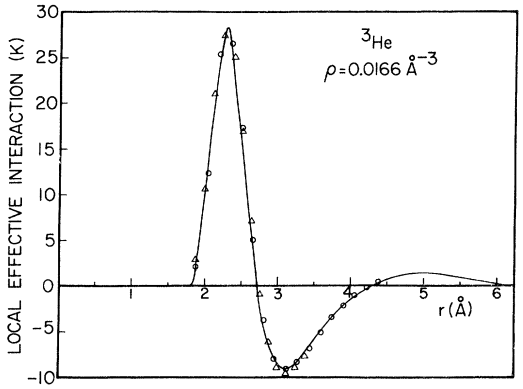

FIG. 2. Local effective interaction in unpolarized ^{3}He as a function of separation. The solid curve traces the Jackson-Feenberg version $\Gamma'_{dd}(r)+(\hbar^2/4m)\nabla^2\Gamma_{dd}(r)$ of this quantity for the SV choice of $f(r)$, while the open circles indicate corresponding results for the Clark-Westhaus version $\Gamma'_{dd}(r)$ [taking account of the effect of the three-body part of the CW kinetic-energy operator (Refs. 19 and 20)]. The triangles mark the JF results for the optimal $f(r)$.

An alternative path may be delineated thus: first recast the CBF perturbation $H_{m0}-H_{00}N_{m0}$ in the form

$$\left\{\frac{[1-\tilde{X}_{cc}(p_1)][1-\tilde{X}_{cc}(p_2)]}{[1-\tilde{X}_{cc}(h_1)][1-\tilde{X}_{cc}(h_2)]}\right\}^{1/2} R(h_1h_2p_1p_2)\ ;$$

then expand the factor $R(h_1h_2p_1p_2)$. That is, expand $\mathfrak{W}^B(12)$ and $\mathfrak{N}^B(12)$ *divided by* $[1-\tilde{X}_{cc}(p_1)]\times[1-\tilde{X}_{cc}(p_2)]$. The simplest approximation within this alternative scheme, labeled $\{\alpha a\}$, retains only the leading term in the expansion of R, i.e., $\mathfrak{W}^B(12)$ and $\mathfrak{N}^B(12)$ are replaced by their local parts and the denominators $[1-\tilde{X}_{cc}(p)]$ of R are set to unity. In all other respects the computation runs as in approximation $\{\alpha\}$ specified above; thus, $\{\alpha a\}$ will differ from $\{\alpha\}$ simply in the presence of an additional factor $\{[1-\tilde{X}_{cc}(p_1)][1-\tilde{X}_{cc}(p_2)]\}^2$ in the integrand of the working formula for $\delta\mathcal{E}^{(2,2)}$. One may in like manner set up an alternative approximation $\{\beta a\}$ corresponding to $\{\beta\}$—by retaining separable diagrams of the type displayed in Eqs. (20) and (21). This amounts in our approximation (i.e., including one-Γ_{dd}-line separable diagrams) to the replacement of $1+\tilde{E}_{ecc}(p_i,h_i)$ by $1+\tilde{X}_{cc}(p_i)+\tilde{E}_{ecc}(p_i,h_i)$ in Eq. (20) and correspondingly in Eq. (21). We see that the contributions of the separable diagrams in the "a" expansion vanish in the zero-momentum-transfer limit. Additional support for the a scheme comes from the fact that, upon carrying on with the a expansion, the average of $R(h_1h_2p_1p_2)$ over hole states will successively approximate the optimization condition $\tilde{\omega}(k)=0$ [cf. (24)]; moreover, some analytical cancellation between central and the average of noncentral effective interactions takes place.

We observe in Tables II and III that all these treatments of the correction $\delta\mathcal{E}^{(2,2)}$ to the $\nu=2$ Jastrow energy yield results of reasonable size. These results depart markedly from those of Table II of CKP, which are invalidated by a programming error. (Here it should be stressed that, in contrast to CKP, the denominator D was *not* replaced by 1 in any of the present calculations.) The entries $\delta\mathcal{E}_{\rm MC}^{(2,2)}\{\beta\}$, corresponding to what we consider the most complete and precise evaluation, are taken as standard; henceforth they will often be denoted simply $\delta\mathcal{E}^{(2,2)}$.

One motivation for the neglect of $u(p)$ numerator terms in approximations $\{\alpha_0\}$, $\{\alpha\}$, and $\{\alpha a\}$ is that $u(k)$ damps toward zero as k increases, ultimately becoming negligible compared to $t(k)$. [A similar rationalization can be given for setting $\tilde{X}_{cc}(p)=0$ in the denominator of $R(h_1h_2p_1p_2)$, since $\tilde{X}_{cc}(k)$ also damps to zero for large k.] Our results show that $\{\alpha\}$ is not a very good approximation when $f_{\rm SV}$ is used; it is much better for optimal correlations. Of course, in the latter case the $u(p)$ terms lead to a singularity at the Fermi surface, so if they are included at all they must be accompanied by counter terms from the basic-diagram expansion of $\mathfrak{W}^B(12)$. We see that in the $f_{\rm opt}$ case the *overall* effect of $u(p)$ numerator terms and nonlocal separable-diagram contributions from the $\mathfrak{W}^B$ expansion is rather modest. Regarding the alternative a evaluations, we take encouragement from the finding that $\delta\mathcal{E}_{\rm MC}^{(2,2)}\{\beta a\}$, calculated for $f_{\rm opt}$, does not deviate greatly from its correspondent $\delta\mathcal{E}_{\rm MC}^{(2,2)}\{\beta\}$; the difference between the $\{\beta a\}$ and $\{\beta\}$ results may be taken as an estimate of the effect of neglected separable diagrams.

It is interesting that the angle-average values $\delta\mathcal{E}_{\rm AA}^{(2,2)}\{\alpha_0\}$ are in fairly close accord with $\delta\mathcal{E}_{\rm MC}^{(2,2)}\{\alpha\}$, which should be the case if the operations (i)–(iii) of the treatment (a) of Sec. II C are justified. However, we infer from the results $\delta\mathcal{E}_{\rm MC}^{(2,2)}\{\alpha\}$ in Table II that the degree of such agreement is enhanced by partial cancellation of errors due to (i)–(ii) by errors due to (iii). One other technical point is of some interest. A comparison, for $f_{\rm SV}$, of the "local effective interactions" $\Gamma'_{dd}(r)+(\hbar^2/4m)\times\nabla^2\Gamma_{dd}(r)$ and $\Gamma'_{dd}(r)$ of JF and CW formulations, respectively, shows them to be in excellent numerical agreement, as seen in Fig. 2. This concurrence lends further credibility to our evaluation of the perturbation correction $\delta\mathcal{E}^{(2,2)}$. For completeness, we also compare, in Fig. 2, the JF local effective interactions for SV and optimal correlations; Fig. 3 displays the function $\Gamma_{dd}(r)$ associated with each of these two choices of $f(r)$.

Turning now to matters of broader concern—in particular, the confrontation of our theoretical results on unpolarized ^{3}He with experiment—we remind the reader that the function of CBF perturbation theory is to correct the (Jastrow) variational energy for the

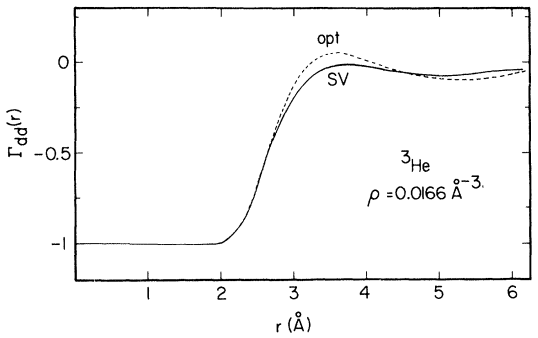

FIG. 3. "Dressed correlation line" $\Gamma_{dd}(r)$ in unpolarized ^{3}He as a function of separation. The solid curve corresponds to the SV choice of $f(r)$, the dashed curve to the optimal choice.

inadequacies of the (Jastrow) trial ground-state wave function. Thus, if $f_{\rm opt}$ as determined here is actually the "best" two-body correlation function (or nearly so) we would expect $\delta\mathcal{E}^{(2,2)}$ to be smaller in magnitude for $f_{\rm opt}$ than for $f_{\rm SV}$. Such is indeed the case; moreover the difference

$$\delta\mathcal{E}^{(2,2)}[f_{\rm opt}]-\delta\mathcal{E}^{(2,2)}[f_{\rm SV}]$$

is a smooth, monotonically increasing function of density, ranging from 0.05 K at $\rho=0.0076$ Å^{-3} to 0.80 K at $\rho=0.020$ Å^{-3}. [Inspecting Figs. 2 and 3, we attribute this difference to differences in $\Gamma_{dd}(r)$—which of course enters prominently in the effective perturbation (16), through Eqs. (17) and (19)—rather than in the "local effective interaction."] For either choice of f, the energetic effect of the residual, non-Jastrow correlations (angle, momentum, spin dependent), as represented by the values for $\delta\mathcal{E}_{\rm MC}^{(2,2)}\{\beta\}$ listed in Tables II and III, is substantial. Nevertheless, the correction we calculate is not sufficient to bridge the gap between $\langle H\rangle$ and the measured energy. The experimental energy at saturated vapor pressure, corresponding to $\rho_e=0.0164$ Å^{-3}, is -2.47 K (per particle). Taking $\mathcal{E}_{(1)}=\langle H\rangle_{\rm FHNC/C-JF}+\delta\mathcal{E}^{(2,2)}$ as the improved theoretical estimate of the energy, we find $\mathcal{E}_{(1)}[f_{\rm opt}]=-1.22$ K and $\mathcal{E}_{(1)}[f_{\rm SV}]=-1.71$ K at $\rho=0.0164$ Å^{-3}. As a function of ρ, $\mathcal{E}_{(1)}[f_{\rm opt}]$ reaches a minimum of -1.41 K at $\rho=0.0136$ Å^{-3}; the corresponding numbers for $f_{\rm SV}$ are -1.71 K at $\rho=0.0160$ Å^{-3}. We shall refine these estimates later, upon returning to the question of the accuracy of the FHNC/C approximation.

We note in passing that the convergence of the CBF perturbation expansion is presumably better for $f_{\rm opt}$ than for $f_{\rm SV}$—the effective perturbation is stronger for the former choice, producing a larger $|\delta\mathcal{E}^{(2,2)}|$. However, having only the leading correction term at our disposal, it is not possible to ascertain in either case whether the rate of convergence is rapid enough for the present approach to be viable. The correction $\delta\mathcal{E}^{(2,2)}$ amounts to only a small percentage (some 5–8% at ρ_e) of the Jastrow potential energy $\langle V\rangle$, and a considerably larger percentage (but $\lesssim$25%) of the Jastrow interaction energy $\langle H\rangle-T_F$, where T_F is the ground-state energy of the noninteracting Fermi gas. Of course, neither comparison yields a legitimate measure of convergence of the CBF expansion. It is our judgment—based on what has been learned about the behavior of the effective perturbation itself—that the portion of $\delta\mathcal{E}^{(3)}$ involving at most correlated $3p$-$3h$ excitations will not be negligible, but should not be overwhelming. In this connection it must be recalled that we have not evaluated the full second-order perturbation correction, but only the portion $\delta\mathcal{E}^{(2,2)}$ of it arising from correlated $2p$-$2h$ excitations. The omitted portion $\delta\mathcal{E}^{(2,3)}$ due to correlated $3p$-$3h$ excitations is also negative and would serve to further close the gap between theory and experiment. On proceeding to higher-order perturbation corrections ($\delta\mathcal{E}^{(4)}$, . . .) and/or higher classes of correlated excitation ($4p$-$4h$, . . .), an awkward technical feature of CBF perturbation theory is encountered.[25,26] In a given perturbative order, spurious, unlinked parts will arise which are cancelled by like contributions from *different* orders of the expansion (3). For example, if we examine the correlated $4p$-$4h$ portion of $\delta\mathcal{E}^{(2)}$, we find unlinked contributions with an unphysical dependence on the particle number. These contributions are eradicated by portions of $\delta\mathcal{E}^{(4)}$ involving correlated $2p$-$2h$ excitations and additional sixth-order terms of similar structure. It is difficult to make any useful general statement about the numerical importance of the physical survivors of such cancellations, although we expect that—aside from previously identified pieces of $\delta\mathcal{E}^{(2)}$ and $\delta\mathcal{E}^{(3)}$ (viz., $\delta\mathcal{E}^{(2,2)}$, $\delta\mathcal{E}^{(2,3)}$, $\delta\mathcal{E}^{(3,2)}$, and $\delta\mathcal{E}^{(3,3)}$)—they are unlikely to become significant except at high density.

In view of the uncertainties touched on in the preceding discussions, it would clearly be desirable to go beyond CBF perturbation theory, in effect summing out the important subseries of contributions within the CBF expansion (3). Such a possibility is offered by the CBF-coupled cluster scheme developed in Ref. 26.

Two additional pieces of information help to illuminate still further the current status of many-body theories of the ground-state energetics of unpolarized liquid ^{3}He. First, the Lennard-Jones interaction is known from virtually exact Green's-function Monte Carlo calculations[27] to *underbind* liquid ^{4}He by about 0.5 K at the experimental equilibrium density 0.0219 Å^{-3} when the Axilrod-Teller three-body interaction[28] is taken into account. For liquid ^{3}He at its lower equilibrium density, a corresponding but smaller deficit in binding will be ascribable to use of the

Lennard-Jones potential. [Of course, within this context the energy to be fit by the many-body calculation would be −2.47 K *minus* the positive contribution (perhaps 0.1 K) from the Axilrod-Teller interaction.] Second, studies by Levesque and Lhuillier[29] and independently by Kalos and collaborators[30] indicate that elaboration of the Jastrow ansatz by a triplet-correlation factor $\prod_{i<j<k} f_3(r_{ij}, r_{ik}, r_{jk})$, where the deviation of f_3 from 1 is small unless all three of ijk are close together, can lead to an appreciable lowering of the energy expectation value, by some 0.4 K at $\rho \cong 0.0164$ Å^{-3}. Presently, attention is swinging to the problem of the proper incorporation of momentum-dependent backflow correlations[10,30] and spin-dependent correlations.[31] We believe[24] that our formalism is well suited to the inclusion of these mechanisms, and that their contribution to the energy is already sensibly approximated by $\delta\mathcal{E}^{(2,2)}$. Furthermore, it may be that the refinements of Levesque and Lhuillier and of Kalos and co-workers provide in effect an estimate of the energetic contribution of CBF $3p$-$3h$ excitations.

Our results on the helium systems are summarized in Figs. 4 and 5. The relative stability of ^{3}He↑ and unpolarized ^{3}He, within the Jastrow model, remains essentially as reported in CKP, i.e., beyond some rather low density, $\langle H \rangle$ for $\nu = 1$ lies *below* that for $\nu = 2$, the difference *widening* with increasing ρ. This artificial behavior is due, of course, to the inadequacy, for the *unpolarized* system, of the simple correlation ansatz $F = \prod_{i<j} f(r_{ij})$—a description which becomes less and less realistic as the density rises. Upon supplementing $\langle H \rangle_{\rm JF}(\nu = 2)$ by $\delta\mathcal{E}^{(2,2)}$ as determined above, the energy estimate for unpolarized ^{3}He is pushed (safely) beneath that of the spin-aligned system, in the case of Schiff-Verlet correlations. For our "optimal" correlations, the stability picture, though also greatly improved, is not fully rectified—the onset of artificial instability being raised from $\rho \approx 0.0105$ to ≈ 0.0150 Å^{-3}. Strictly, these comparisons are not consistent—one should also augment $\langle H \rangle_{\rm JF}(\nu = 1)$ with its $\delta\mathcal{E}^{(2,2)}$. Still, as argued in the Introduction, the latter quantity (or more precisely the correction to the Jastrow energy) is likely to be quite small. (Note that there is simply not much room between the Jastrow $\langle H \rangle$ for $\nu = 1$ and the exact energy of this system, which is expected to lie a few tenths of a degree above that for the unpolarized liquid.)

To gauge the accuracy of the FHNC/C evaluation of $\langle H \rangle$, several data points extracted from the "benchmark" variational Monte Carlo results of Levesque[11] have been included in Fig. 4. (For the unpolarized phase, Levesque does not give $\langle H \rangle$ values corresponding to the parameter choice $b = 1.13\sigma$; modest interpolation or extrapolation of his results was required in that case. Quoted statistical errors are typically ±0.15 for the $\nu = 2$ system and

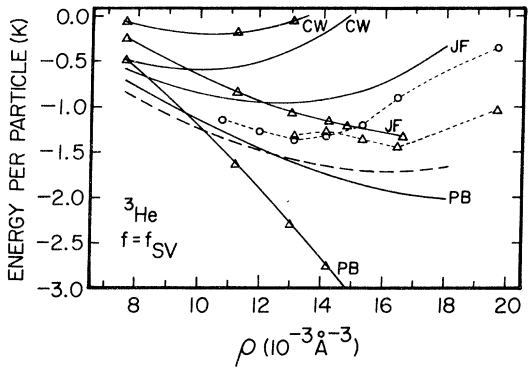

FIG. 4. Ground-state energy per particle vs density for unpolarized and fully polarized ^{3}He, based on the Lennard-Jones potential and the Schiff-Verlet correlation function $f_{\rm SV}(r) = \exp[-\frac{1}{2}(b/r)^5]$ with $b = 2.888$ Å. *Solid curves without data points:* Jastrow energy expectation value $\langle H \rangle$ for *unpolarized* ^{3}He, computed in FHNC/C approximation using (as labeled) CW, JF, and PB expressions for the kinetic energy. *Solid curves with triangle data points:* Jastrow energy expectation value for *fully polarized* ^{3}He computed in FHNC/C approximation. *Short-dash lines* connect Monte Carlo data points of Levesque (Ref. 11) for $\langle H \rangle$, designated by *open circles* (unpolarized ^{3}He) and *triangles* (fully polarized ^{3}He). *Long-dash curve:* CBF estimate of ground-state energy of *unpolarized* system, formed by adding the second-order perturbation correction $\delta\mathcal{E}^{(2,2)}$ to $\langle H \rangle_{\rm JF}$(FHNC/C).

±0.20 for $\nu = 1$.) The FHNC/C curves for $\langle H \rangle_{\rm JF}$ lie somewhat above the respective Monte Carlo (MC) results, the discrepancy being unimportant for the polarized system (i.e., within the numerical error bars) and some 0.2–0.4 K in the unpolarized case. (It is interesting that this comparison does not reveal a pronounced increase of the discrepancy with

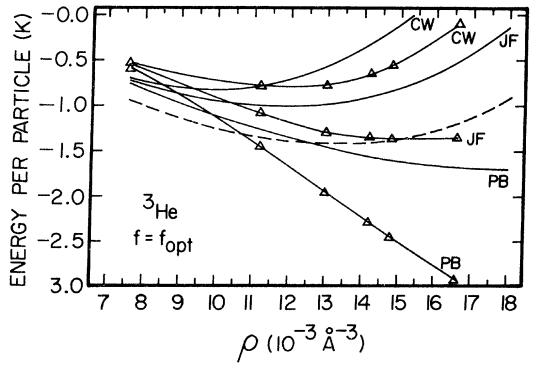

FIG. 5. Ground-state energy per particle vs density of unpolarized and fully polarized ^{3}He, based on the Lennard-Jones potential and the optimally determined correlation function, $f_{\rm opt}(r)$. Notation as in Fig. 4, except that Monte Carlo results for $\langle H \rangle$ are not available for comparison in the present case.

density—which one would expect to see if the elementary-diagram contribution is growing rapidly.) Taking the Levesque results as accurate, a refined CBF estimate of the energy may be formed, viz., $\mathcal{E}_{(2)} = \langle H \rangle_{\rm MC} + \delta\mathcal{E}^{(2,2)}$. For SV correlations we then obtain, at $\rho = 0.0164$ Å$^{-3} = \rho_e$, the value $\delta\mathcal{E}_{(2)} = -1.95$ K. Reasoning that for truly optimal correlations and accurately evaluated expectation values $\langle H \rangle[f_{\rm opt}]$ will be less than $\langle H \rangle[f_{\rm SV}]$, and assuming that the $\delta\mathcal{E}^{(2,2)}$ evaluation of Table III remains valid, we may quote -1.56 K as an upper bound to $\mathcal{E}_{(2)}$ for the optimal $f(r)$. These revised theoretical estimates improve on our earlier comparison with experiment; indeed $\mathcal{E}_{(2)}[f_{\rm SV}]$ brings us within striking distance of the measured energy. Use of Levesque's benchmarks in conjunction with the CBF correction $\delta\mathcal{E}^{(2,2)}$ also distinctly improves the theoretical situation in the SV case with regard to the relative stability of polarized and unpolarized phases, since $\langle H \rangle_{\rm FHNC/C-JF} - \langle H \rangle_{\rm MC}$ is larger for $\nu = 2$ than 1.

B. Deuterium systems

In our investigations of the deuterium systems $D\downarrow_1$, $D\downarrow_2$, and $D\downarrow_3$ we adopt the accurate theoretical pair potential for the $b^3\Sigma_u^+$ state which has been constructed by Kolos and Wolniewicz.[32] Calculations were performed for Pandharipande-Bethe correlation functions[8] $f_{\rm PB}$ as well as Schiff-Verlet and optimal choices. The parameter b in $f_{\rm SV}$ was determined at *each* ν and *each* ρ by minimization of $\langle H \rangle_{\rm JF}$. [Actually, for $D\downarrow_1$ and $D\downarrow_2$ we have used $b(\nu, \rho)$ as supplied by M. D. Miller, after checking that his values minimize, or nearly minimize, $\langle H \rangle_{\rm JF}$ as approximated here.] Otherwise our deuterium studies run essentially parallel to those detailed above for ^{3}He. The main numerical results are collected in Tables IV–VII and summarized (for the $f_{\rm opt}$ case) in Fig. 6. For the most part, the features and trends seen in these results echo those noted for the helium systems. Thus, much of the discussion of Sec. III A could be repeated here, with $D\downarrow_2$ (or $D\downarrow_3$) playing the role of unpolarized ^{3}He and $D\downarrow_1$ that of ^{3}He$\uparrow$. Let us instead concentrate on the novel aspects of the deuterium problem which emerge from our results.

Table IV and Fig. 7 extend the study of the deuterium systems with the SV correlation function[2] to $D\downarrow_3$, the case of three equally populated nuclear spin states. At very low density, there is very close agreement among $\langle H \rangle_{\rm CW}$, $\langle H \rangle_{\rm JF}$, and $\langle H \rangle_{\rm PB}$. As the density increases, the spread between the three forms of the energy expectation value grows, but not nearly so fast as with ^{3}He. This suggests that the elementary diagrams are less important for deuterium.

Examining the JF entries in Tables IV–VI for $D\downarrow_2$ and $D\downarrow_3$, we find that the PB and optimal choices of f yield an energy expectation value $\langle H \rangle$ which is

TABLE IV. Jastrow ground-state energies of deuterium systems for $f_{\rm SV}$. Energies in K per particle. Entries marked with an asterisk are from the calculation of Ref. 2.

		$D\downarrow_1$				$D\downarrow_2$				$D\downarrow_3$			
ρ (10^{-3} Å^{-3})	$\rho\sigma^3$	b	$\langle H \rangle_{\rm CW}$	$\langle H \rangle_{\rm JF}$	$\langle H \rangle_{\rm PB}$	b	$\langle H \rangle_{\rm CW}$	$\langle H \rangle_{\rm JF}$	$\langle H \rangle_{\rm PB}$	b	$\langle H \rangle_{\rm CW}$	$\langle H \rangle_{\rm JF}$	$\langle H \rangle_{\rm PB}$
1.41	0.071	3.681	0.48	0.49	0.49	3.872	0.28	0.28	0.27	3.913	0.13	0.13	0.12
2.82	0.142	3.752	0.42	0.33	0.23	3.901	0.32	0.26	0.18	3.930	0.15	0.09	0.03
3.52	0.177	3.781	0.49	0.30	0.06	3.917	0.47	0.33	0.17	3.951	0.29	0.17	0.04
4.23	0.213	3.818	0.68	0.30	−0.14	3.938	0.74	0.48	0.20	3.967	0.57	0.35	0.10
4.93	0.248	3.839	1.03	0.39	−0.37	3.951	1.18	0.75	0.28	3.984	1.00	0.63	0.22
5.63	0.283	3.864	1.49	0.56	−0.58	3.963	1.78	1.12	0.41	4.000	1.67	1.07	0.45
6.34	0.319	3.884	2.12*	0.75*	−0.86*	3.980	2.60*	1.63*	0.58*	4.017	2.54	1.65	0.73
7.04	0.354	3.926	2.99*	1.04*	−1.25*	3.988	3.63*	2.28*	0.83*	4.033	3.67	2.40	1.09

TABLE V. Jastrow ground-state energies of deuterium systems for f_{PB}, with $d/r_0=2.2$. Energies in K per particle.

ρ (10^{-3} Å^{-3})	$\rho\sigma^3$	$\langle H\rangle_{CW}$	D$\downarrow_1$ $\langle H\rangle_{JF}$	$\langle H\rangle_{PB}$	$\langle H\rangle_{CW}$	D$\downarrow_2$ $\langle H\rangle_{JF}$	$\langle H\rangle_{PB}$	$\langle H\rangle_{CW}$	D$\downarrow_3$ $\langle H\rangle_{JF}$	$\langle H\rangle_{PB}$
1.41	0.071	0.47	0.49	0.51	0.24	0.24	0.24	0.10	0.11	0.11
2.82	0.142	0.44	0.35	0.27	0.25	0.20	0.15	0.09	0.05	0.02
3.52	0.177	0.52	0.31	0.09	0.38	0.26	0.15	0.21	0.11	0.01
4.23	0.213	0.72	0.32	−0.13	0.64	0.41	0.17	0.47	0.28	0.09
4.93	0.248	1.06	0.40	−0.35	1.06	0.68	0.29	0.89	0.59	0.28
5.63	0.283	1.55	0.53	−0.64	1.65	1.08	0.49	1.51	1.03	0.52
6.34	0.319	2.19	0.79	−0.83	2.45	1.61	0.73	2.35	1.61	0.85
7.04	0.354	3.00	1.10	−1.12	3.47	2.29	1.07	3.42	2.42	1.38

generally lower than for the SV choice. However, the difference is less than the estimated numerical uncertainty (~0.1 K) arising from the limited number of grid points. In the case of D$\downarrow_1$, f_{opt} gives a slight energetic improvement over f_{PB} and f_{SV}, except at the highest densities. We note that the SV choice for f seems to serve well for the deuterium systems, as it does in helium.

Energy curves for D$\downarrow_1$, D$\downarrow_2$, and D$\downarrow_3$ based on the optimal choice of f are displayed in Fig. 6. The predicted locations of the finite-density energy minima are 3.7×10^{-3} Å^{-3} (D$\downarrow_1$) and 3.0×10^{-3} Å^{-3} (D$\downarrow_2$ and D$\downarrow_3$), when the CBF perturbation correction is included in the energy estimates for D$\downarrow_2$ and D$\downarrow_3$.

In *concert* with our findings on the effects of nuclear-spin polarization in ^{3}He, the Jastrow model predicts that fully spin-polarized deuterium D$\downarrow_1$ would be preferred over the partially polarized state D$\downarrow_2$ and the spin-saturated state D$\downarrow_3$ above some relatively low density. Again, this may be taken as an indication of the inadequacy of the simple correlation ansatz (2) for $\nu>1$. Over most of the density range of Fig. 6, the results for D$\downarrow_2$ and D$\downarrow_3$ exhibit a physically more realistic behavior with respect to one another: at a given ρ, $\langle H\rangle(\nu=3)$ lies below $\langle H\rangle(\nu=2)$. Nevertheless, at high density the D$\downarrow_2$ curve drops below the curve for D$\downarrow_3$. Qualitatively, the differences between the energy curves for D$\downarrow_2$ and D$\downarrow_3$ are not as prominent as between either D$\downarrow_2$ or D$\downarrow_3$ and D$\downarrow_1$. This is in line with the observation that the ν dependence enters the calculations essentially as ν^{-1}, which makes a smaller "jump" as ν changes from 3 to 2 as compared to the change from 3 or 2 to 1.

In *contrast* to our findings for polarized and unpolarized liquid helium, the *equilibrium* ($d\mathcal{E}/d\rho=0$) results of the Jastrow model for D$\downarrow$ are consistent with expectations based on elementary physical arguments[33] in that the (finite-density) minimum of $\langle H\rangle$ vs ρ for $\nu=3$ lies below that for $\nu=2$, which in turn lies below the minimum for $\nu=1$.

Table VII collects data on $\delta\mathcal{E}^{(2,2)}$ for D$\downarrow_{2,3}$, obtained with the optimal choice of f. For reasons stated in Sec. I, no results are reported for $\nu=1$ at this time. As with unpolarized ^{3}He, the current values of $\delta\mathcal{E}^{(2,2)}$ for D$\downarrow_2$ are markedly different from those quoted in Ref. 2; the results in Table VII may be considered reliable. Inspection of Table VII reveals that $|\delta\mathcal{E}^{(2,2)}(\nu=2)|$ is *larger* than $|\delta\mathcal{E}^{(2,2)}(\nu=3)|$. Consequently, when added to $\langle H\rangle_{JF}$ from Table VI

TABLE VI. Jastrow ground-state energies of deuterium systems for f_{opt}. Energies in K per particle.

ρ (10^{-3} Å^{-3})	$\rho\sigma^3$	$\langle H\rangle_{CW}$	D$\downarrow_1$ $\langle H\rangle_{JF}$	$\langle H\rangle_{PB}$	$\langle H\rangle_{CW}$	D$\downarrow_2$ $\langle H\rangle_{JF}$	$\langle H\rangle_{PB}$	$\langle H\rangle_{CW}$	D$\downarrow_3$ $\langle H\rangle_{JF}$	$\langle H\rangle_{PB}$
1.41	0.071	0.41	0.43	0.45	0.22	0.23	0.23	. . .	. . .	. . .
2.82	0.142	0.32	0.29	0.23	0.25	0.21	0.16	0.09	0.05	0.00
3.52	0.177	0.37	0.24	0.07	0.39	0.28	0.15	0.23	0.12	−0.00
4.23	0.213	0.54	0.26	−0.09	0.66	0.43	0.18	0.52	0.30	0.05
4.93	0.248	0.84	0.35	−0.26	1.10	0.70	0.25	0.97	0.57	0.14
5.63	0.283	1.31	0.55	−0.43	1.74	1.10	0.38	1.69	1.03	0.37
6.34	0.319	1.97	0.83	−0.61	2.62	1.66	0.58	2.63	1.65	0.61
7.04	0.354	. . .	. . .	. . .	3.76	2.35	0.79	3.88	2.47	0.97

TABLE VII. Perturbation correction in deuterium systems, for $f_{\rm opt}$. Energies in K per particle.

ρ (10^{-3} Å^{-3})	$D\downarrow_2$ $\delta\mathcal{E}^{(2,2)}\{\beta\}$	$D\downarrow_3$ $\delta\mathcal{E}^{(2,2)}\{\beta\}$
1.41	−0.07 ±0.004	. . .
2.82	−0.15 ±0.01	−0.13 ±0.01
3.52	−0.20 ±0.01	−0.18 ±0.01
4.23	−0.27 ±0.01	−0.24 ±0.01
4.93	−0.34 ±0.02	−0.30 ±0.02
5.63	−0.43 ±0.02	−0.37 ±0.02
6.34	−0.55 ±0.02	−0.45 ±0.02
7.04	−0.69 ±0.03	−0.54 ±0.03

to form a CBF estimate of the energy, $\mathcal{E} = \langle H\rangle_{\rm JF} + \delta\mathcal{E}^{(2,2)}$, the energy curve for $D\downarrow_2$ drops below that for $D\downarrow_3$ at a lower density than when $\langle H\rangle_{\rm JF}$ alone is used. The ordering of equilibria mentioned above, i.e., $\min\mathcal{E}(\nu=3) < \min\mathcal{E}(\nu=2)$, is, however, preserved.

Finally, we address once again the question of whether spin-aligned deuterium will be found to be a gas or a liquid at $T=0$ and zero external pressure. Based on the minima of the curves corresponding to our best estimates of the energy, $D\downarrow_3$ would be a liquid, $D\downarrow_2$ and $D\downarrow_1$ being gases, even at $T=0$. However, since we have calculated only the $2p$-$2h$ contribution to the second-order correction, there remains the distinct possibility that $D\downarrow_2$ is also a liquid in its absolute ground state. Further, were it to be the case for deuterium, contrary to expectations for liquid ^{3}He, that $\delta\mathcal{E}^{(2,2)}(\nu=1) < \delta\mathcal{E}^{(2,2)}(\nu=2,3)$, then even fully spin-polarized deuterium $D\downarrow_1$ may turn out to have a liquid ground state. We point out that if in fact the energy versus density curve for any of the three examples fails to dip below zero, the energy at the finite-density minimum will still be so small that a very modest pressure will suffice to liquefy the system.

The above predictions concerning the ground-state phase are made against a background of serious complications. We have just referred to the fact that the Jastrow energies are extremely small, as a result of near cancellation of large kinetic and potential energy terms. Consequently, in some cases, the magnitude of $\langle H\rangle$ is less than the numerical uncertainty of the calculation. The differences among $\langle H\rangle_{\rm CW}$, $\langle H\rangle_{\rm JF}$, and $\langle H\rangle_{\rm PB}$ are also of the order of this uncertainty in the vicinity of the minima of the energy curves. It would be helpful, therefore, to have Monte Carlo benchmarks for the deuterium systems, similar to those available for helium,[11,27,29,30] that would allow us to assess the accuracy of the FHNC and CBF schemes. We might then proceed to a more confi-

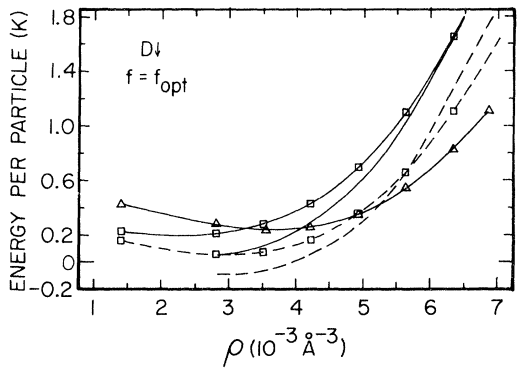

FIG. 6. Ground-state energy per particle vs density for three species of electron-spin-aligned deuterium, based on the Kolos-Wolniewicz potential and the optimally determined correlation function, $f_{\rm opt}(r)$. *Solid curve with triangle data points:* Jastrow energy expectation value $\langle H\rangle$ for $D\downarrow_1$ (one nuclear spin state present), computed in FHNC/C approximation using the JF expression for the kinetic energy. *Solid curve with square data points:* same but for $D\downarrow_2$ (two equally populated nuclear spin states). *Solid curve without data points:* same but for $D\downarrow_3$ (three equally populated nuclear spin states). *Long-dash curve with square data points:* CBF estimate of ground-state energy of $D\downarrow_2$, formed by adding the second-order perturbation correction $\delta\mathcal{E}^{(2,2)}$ to $\langle H\rangle_{\rm JF}$ (FHNC/C). *Long-dash curve without data points:* corresponding CBF estimate for $D\downarrow_3$.

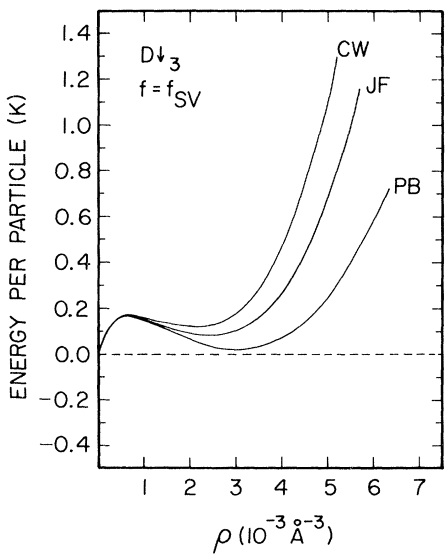

FIG. 7. Ground-state energy per particle vs density for the electron-spin-aligned deuterium system $D\downarrow_3$ with three equally populated nuclear spin states, based on the Kolos-Wolniewicz potential and the Schiff-Verlet correlation function $f_{\rm SV}(r)$. Solid curves: Jastrow energy expectation value computed in FHNC/C approximation, using (as labeled) CW, JF, and PB expressions for the kinetic energy.

dent prediction of ground-state phase and other properties of the deuterium systems at zero temperature. It should be stressed that the atom-atom interaction in deuterium is very accurately known; compared to the situation in nuclear matter or even liquid ^{3}He, the two-body potential introduces negligible uncertainty into the problem. Spin-aligned deuterium offers, therefore, both an outstanding computational challenge to many-body theorists and a new proving ground for the predictive power of many-fermion theories.

APPENDIX A: EULER AND FNHC′ EQUATIONS

An Euler equation for the Jastrow wave function (2) has been derived previously by one of us (Ref. 14). The aim of that work was, however, to uncover properties of the solution of the exact variational problem (5), free from the imposition of any cluster-expansion or -resummation treatment. Moreover, the CW expression for the energy expectation value, rather than the JF representation, was employed.

A derivation tailored to the present, computational, effort proceeds as follows. Appealing to the Jackson-Feenberg identity (11), the energy expectation value may be cast in the JF form:

$$H_{00}=\langle\Phi_0|F^\dagger HF|\Phi_0\rangle I_{00}^{-1}$$
$$=T_F+I_{00}^{-1}\int d\tau_1\cdots d\tau_A F^2(1\cdots A)\times\left[\sum_{i<j}v_{\rm JF}(r_{ij})+\frac{\hbar^2}{8m}\sum_i\nabla_i^2\right]|\Phi_0(1\cdots A)|^2 \quad \text{(A1)}$$

Here, I_{00} is the squared norm of the Jastrow ground-state trial function, $T_F=(3\hbar^2k_F^2/10m)A$ is the kinetic energy of the noninteracting Fermi gas, $\int d\tau_i$ stands both for integration over the spatial coordinates and summation over the spin variable of particle i, $i=1,\ldots,A$, and $v_{\rm JF}$ is the Jackson-Feenberg effective interaction

$$v_{\rm JF}(r)=v(r)-(\hbar^2/4m)\nabla^2u(r)\ . \quad \text{(A2)}$$

in which $\mathbf{u}(r)\equiv\ln f^2(r)$. It is quite straightforward to generate an Euler equation based on this energy functional (cf. Ref. 14). We obtain

$$0=\left[\frac{\delta H_{00}[f]}{\delta\mathbf{u}}\right](r)=-(\hbar^2/4m)\nabla^2g(r)+g'(r)\ , \quad \text{(A3)}$$

where $g(r)$ is the familiar radial distribution function and $g'(r)$ is a generalized distribution function defined by

$$g'(r)=I_{00}^{-1}\frac{A(A-1)}{\rho^2}\int d\tau_3\cdots d\tau_A F^2(1\cdots A)\times\left[\sum_{i<j}v_{\rm JF}(r_{ij})+\frac{\hbar^2}{8m}\sum_i\nabla_i^2\right]|\Phi_0(1\cdots A)|^2-g(r)(H_{00}-T_F) \quad \text{(A4)}$$

One may note that the $\nabla^2g(r)$ term in Eq. (A3) comes from variation of the JF effective interaction (A2) with respect to $\mathbf{u}(r)$, whereas the $g'(r)$ term arises from the dependence on $\mathbf{u}(r)$ of the radial distribution functions involved in the energy expectation value. Transforming Eq. (A3) to Fourier space, and denoting the Fourier transform of $g'(r)$ by $S'(k)$, we arrive at Eq. (6).

The distribution function $g(r)$ entering Eq. (A3), or alternatively the structure function $S(k)$ in Eq. (6), may be dealt with by means of FHNC theory. Our task is evidently not complete without a parallel analysis, and reduction to calculable form, of the primed counterparts $g'(r)$ and $S'(k)$ of $g(r)$ and $S(k)$. The formulation of FHNC-type equations for these quantities is most expeditiously achieved via the functional differentiation procedure of Ref. 19 (see also Feenberg[12]), although for formal considerations it is advisable also to keep in mind the diagrammatic content of the various quantities which come into play. In analogy with the non-nodal X sets and nodal N sets of the FHNC diagrammatic analysis[6] of $g(r)$, one is led to introduce X' sets and N' sets of $g'(r)$ diagrams. However, whereas X_{ij} and N_{ij} diagrams (with $ij=dd$, de, ee, or cc in the now-conventional notation[6]) are individually composed of dynamical correlation bonds $f^2(r_{ab})-1$ and exchange bonds $l(k_Fr_{ab})$ alone, their primed counterparts also involve exactly one of the following: (i) an effective interaction line $f^2(r_{ab})v_{\rm JF}(r_{ab})$, (ii) a differentiated exchange line $(\hbar^2/2m)\nabla^2l(k_Fr_{ab})$, or (iii) a connected pair of differentiated exchange lines $(\hbar^2/2m)\nabla_al(k_Fr_{ab})\cdot\nabla_al(k_Fr_{ac})$.

Graphical analysis or simple functional differentiation,

$$S'(k)=\sum_{mn}\frac{\delta S(k)}{\delta\tilde{X}_{mn}(k)}\tilde{X}'_{mn}(k)\ ,$$
$$\tilde{N}'_{ij}(k)=\sum_{mn}\frac{\delta\tilde{N}_{ij}(k)}{\delta\tilde{X}_{mn}(k)}\tilde{X}'_{mn}(k)\ , \quad \text{(A5)}$$

leads to these explicit equations in terms of primed X's and quantities known from FHNC analysis[2,6]:

$$S'(k)=S^2(k)\tilde{X}'_{dd}(k)+2S(k)S_d(k)\tilde{X}'_{de}(k)+S_d^2(k)\tilde{X}'_{ee}(k) \ , \tag{A6}$$

$$\tilde{N}'_{dd}(k)=[S_d^2(k)-1]\tilde{X}'_{dd}(k)+2\tilde{\Gamma}_{dd}(k)S_d(k)\tilde{X}'_{de}(k)+\tilde{\Gamma}_{dd}^2(k)\tilde{X}'_{ee}(k) \ , \tag{A7}$$

$$\begin{aligned}\tilde{N}'_{de}(k)=&S_d(k)[S(k)-S_d(k)]\tilde{X}'_{dd}(k)\\&+\{\tilde{\Gamma}_{dd}(k)[S(k)-S_d(k)]+S_d(k)[S_d(k)-\tilde{\Gamma}_{dd}(k)]-1\}\tilde{X}'_{de}(k)\\&+\tilde{\Gamma}_{dd}(k)[S_d(k)-\tilde{\Gamma}_{dd}(k)]\tilde{X}'_{ee}(k) \ ,\end{aligned} \tag{A8}$$

$$\begin{aligned}\tilde{N}'_{ee}(k)=&[S(k)-S_d(k)]^2\tilde{X}'_{dd}(k)+2[S(k)-S_d(k)][S_d(k)-\tilde{\Gamma}_{dd}(k)]\tilde{X}'_{de}(k)\\&+\{[S_d(k)-\tilde{\Gamma}_{dd}(k)]^2-1\}\tilde{X}'_{ee}(k) \ ,\end{aligned} \tag{A9}$$

$$\tilde{N}'_{cc}(k)=\{[1-\nu^{-1}\tilde{l}(k)]/[1-\tilde{X}_{cc}(k)]^2-1\}\tilde{X}'_{cc}(k) \ . \tag{A10}$$

We have introduced the abbreviation

$$S_d(k)=\{1+[1+\tilde{X}_{ee}(k)]\tilde{\Gamma}_{dd}(k)\}/[1-\tilde{X}_{de}(k)] \ . \tag{A11}$$

In a similar manner we may in turn construct r-space equations for the sums X'_{ij} of the X' sets of diagrams:

$$X'_{dd}(r)=[1+\Gamma_{dd}(r)][v_{\rm JF}(r)+E'_{dd}(r)]+\Gamma_{dd}(r)N'_{dd}(r) \ , \tag{A12}$$

$$X'_{de}(r)=\Gamma'_{dd}(r)[N_{de}(r)+E_{de}(r)]+[1+\Gamma_{dd}(r)]E'_{de}(r)+\Gamma_{dd}(r)N'_{de}(r) \ , \tag{A13}$$

$$\begin{aligned}X'_{ee}(r)=&\Gamma'_{dd}(r)\{-\nu^{-1}L^2(r)+[N_{de}(r)+E_{de}(r)]^2+N_{ee}(r)+E_{ee}(r)\}\\&+2[1+\Gamma_{dd}(r)]\{L(r)N'_{cc}(r)+[N_{cc}(r)+E_{cc}(r)][N'_{cc}(r)+E'_{cc}(r)]+E'_{ee}(r)\}\\&+\Gamma_{dd}(r)N'_{ee}(r)-(\hbar^2/2m)[1+\Gamma_{dd}(r)]\{L(r)\nabla^2 l(k_Fr)+[\nabla l(k_Fr)]^2\} \ ,\end{aligned} \tag{A14}$$

$$X'_{cc}(r)=-\nu^{-1}\{\Gamma'_{dd}(r)L(r)+[1+\Gamma_{dd}(r)]E'_{cc}(r)\}+\Gamma_{dd}(r)[N'_{cc}(r)-(\hbar^2/4m)\nabla^2 l(k_Fr)] \ , \tag{A15}$$

wherein the $E_{ij}(ij=dd,\ de,\ ee,\ cc)$ are the corresponding sums of elementary diagrams, $\Gamma'_{dd}(r)=X'_{dd}(r)+N'_{dd}(r)$, and

$$L(r)\equiv l(k_Fr)-\nu N_{cc}(r) \ . \tag{A16}$$

Equations (A7)–(A10) and (A12)–(A15) comprise what we call the FHNC′ equations. We have not written out additional small contributions to $X'_{ee}(r)$ and $X'_{cc}(r)$ arising from the three-body part of the Jackson-Feenberg effective kinetic energy operator; these terms are, however, included in the numerical computations. The FHNC equations determining the compound-diagrammatic objects X_{ij} and N_{ij} and the functional derivatives required to form $S'(k)$, $\tilde{N}'_{ij}(k)$, and $X'_{ij}(r)$ are well known[2,6] and need not be reproduced here. Still, we should note the definition

$$\Gamma_{dd}(r)\equiv f^2(r)\exp[N_{dd}(r)+E_{dd}(r)]-1$$

and the relation $X_{dd}+N_{dd}=\Gamma_{dd}$. The so-called /0 truncation of the FHNC and FHNC′ equations is obtained by setting all the elementary quantities E_{ij} and E'_{ij} equal to zero.

In our approximation procedures for solution of the FHNC′ equations and optimization of $f(r)$, the free-fermion component of $\tilde{X}'_{ee}(k)$ is singled out for special attention

$$\tilde{X}'_{ee}(k)=-(\hbar^2k^2/4m)[S_F(k)-1]+O(f^2-1) \tag{A17}$$

Here, $S_F(k)$ is the static structure function of the noninteracting system.

The exact long-wavelength behavior of the quantities $\tilde{X}_{de}(k)$ and $\tilde{X}_{ee}(k)$ was established in Ref. 14. It is found that

$$\left.\begin{aligned}\tilde{X}_{de}(k)&=O(k)\\1+\tilde{X}_{ee}(k)&=S_F(k)+O(k^2)\end{aligned}\right\}\ (k\rightarrow 0^+) \ . \tag{A18}$$

These properties may be traced to the Pauli exclusion principle, and are required for the proper long-wavelength behavior of the static structure function, namely, $S(k)=O(k)$, $k\rightarrow 0^+$. Correspondingly, the following low-k behavior of the primed quantities $\tilde{X}'_{de}(k)$ and $\tilde{X}'_{ee}(k)$ may be established:

$$\left.\begin{aligned}\tilde{X}'_{de}(k)&=O(k)\\\tilde{X}'_{ee}(k)&=O(k^2)\end{aligned}\right\}\ (k\rightarrow 0^+) \ . \tag{A19}$$

It is important to note that Eqs. (A18) and (A19) hold not only for the full diagram sums, but also within approximations in which appropriate sets of elementary diagrams are retained. Adherence to these "identities" produces considerable improvement of convergence in iterative treatment of the FHNC and FHNC′ equations, and is in fact indispensible to our optimization procedure. If one is working within the FHNC/n ordering scheme,[6] Eqs.

(A18)–(A19) can, strictly speaking, only be preserved if infinite sums of elementary diagrams are incorporated. Even so, given the /0 approximations to $\tilde{X}_{de}(k)$ and $\tilde{X}_{ee}(k)$ and their primed counterparts, we can adequately simulate the effects of the missing elementary diagrams, so far as the above small-k properties are concerned, by adopting the FHNC/C algorithm,[17]

$$\tilde{X}_{de}^{/C}(k) = S_F(k)\tilde{X}_{de}^{/0}(k) \ ,$$

$$\tilde{X}_{ee}^{/C}(k) = [S_F^2(k)-1]\{\tilde{X}_{ee}^{/0}(k) - [S_F(k)-1]\} + \tilde{X}_{ee}^{/0}(k) \ , \quad \text{(A20)}$$

and similarly

$$\tilde{X}_{de}^{\prime/C}(k) = S_F(k)\tilde{X}_{de}^{\prime/0}(k) \ ,$$

$$\tilde{X}_{ee}^{\prime/C}(k) = S_F^2(k)\{\tilde{X}_{ee}^{\prime/0}(k) + (\hbar^2k^2/4m)[S_F(k)-1]\} - (\hbar^2k^2/4m)[S_F(k)-1] \ . \quad \text{(A21)}$$

For the purpose of computing the Jastrow energy expectation value, the radial distribution function is constructed using Eq. (6) of Ref. 17 rather than by Fourier inversion of $S(k)-1$ derived from the structural relation[2,6,18]

$$S(k) = [1+\tilde{X}_{ee}(k)]S_d(k)/[1-\tilde{X}_{de}(k)] \ . \quad \text{(A22)}$$

The FHNC and FHNC′ equations are handled just as in the /0 scheme, with the sole exception that the $\tilde{X}_{ij}^{/0}(k)$ and $\tilde{X}_{ij}^{\prime/0}(k)$ appearing in the chain equations [i.e., the $\tilde{N}_{ij}^{\prime}(k)$ equations (A7)–(A10) and their unprimed counterparts[2,6]], are "dressed" according to Eqs. (A20) and (A21).

Finally, we should take notice of the fact that the long-wavelength limit of $S'(k)/S^2(k)$,

$$S'(k)/S^2(k)\big|_{k\to 0^+} \equiv \tilde{X}(0^+) + (\hbar^2/4m)[k/S(k)]^2\big|_{k\to 0^+} \ , \quad \text{(A23)}$$

where $\tilde{X}(0^+)$ is composed of FHNC quantities, may be related to Landau's symmetrical Fermi-liquid parameters (see Ref. 14 for detailed expressions). The relation in question presumes, however, that all elementary diagrams are included; thus we can only expect it to be of qualitative value if our calculated results, based on the /C estimates (A20)–(A21), are used for the FHNC ingredients.

Nevertheless, Eq. (A23) provides the key quantity in predicting the long-range component of the Jastrow function $f(r)-1$. From Eq. (6) together with Eq. (A23) we find

$$[S_F(k)/S(k)]^2\big|_{k\to 0^+} = 1 + 9m\tilde{X}'(0^+)/4\hbar^2k_F^2 \ , \quad \text{(A24)}$$

and via the arguments of Ref. 14 we have

$$S(k)/S_F(k) \sim 1 + \nu k_F^2 c_L/4 \quad (k\to 0^+) \quad \text{(A25)}$$

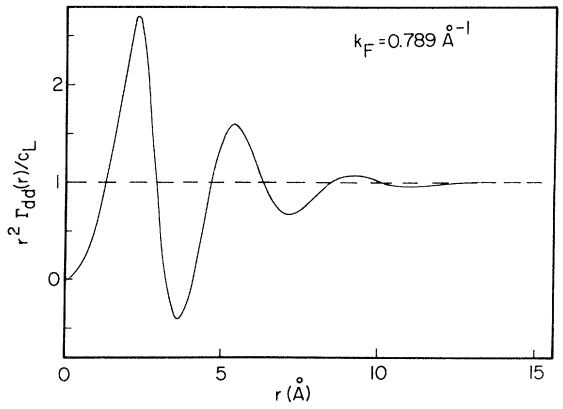

FIG. 8. Solid curve represents the function $r^2\Gamma_{dd}(r)$ in unpolarized ^{3}He as obtained by PPA iteration, measured in units of c_L, the predicted asymptotic ($r\to\infty$) value of this function. The indicated k_F corresponds to $\rho = 0.0166$ Å^{-3}, i.e., essentially the experimental equilibrium density.

for

$$r^2\Gamma_{dd}(r) \sim c_L \quad (r\to\infty) \ . \quad \text{(A26)}$$

In Fig. 8, the asymptotic behavior of $\Gamma_{dd}(r)$ as predicted by means of Eqs. (A24)–(A26) is compared with the behavior of $\Gamma_{dd}(r)$ actually obtained by PPA iteration. The excellent agreement attests to the numerical consistency of our solution of the optimization problem.

APPENDIX B: NUMERICAL OPTIMIZATION

In order to demonstrate the efficiency and stability of our optimization procedure, we have deliberately adopted the simplest of numerical tools. Calculations were performed on an equidistant mesh of 128 points in coordinate space, and likewise in momentum space. All integral equations were solved by iteration, using a linear Filon integration in conjunction with the fast Fourier transform (FFT) method for the evaluation of trigonometric sums.

Considerable savings were accrued by taking $\Gamma_{dd}(r)$ as the unknown function. This obviates the most cumbersome of the FHNC equations and decouples the *cc* equation from the *de* and *ee* equations. At each step of the PPA scheme one constructs $f(r)$ from the updated $\Gamma_{dd}(r)$ and $N_{dd}(r)$.

Some care had to be exercised to avoid spurious numerical results due to finite-box-size effects. Such errors may be caused by a mismatch between the predicted and the calculated asymptotic tail of $f(r)$, or by large weight factors of those correlation components which fall off faster than r^{-2} and cannot be treated analytically.

We should point out that the manner of conver-

gence of the PPA iterations (and in particular of the JF energies corresponding to successive iterations) did not in itself suffice to indicate whether the iterations were converging to a spurious solution, nor did inspection of $g(r)$ or $S(k)$.

In addition to direct examination of the function $r^2\Gamma_{dd}(r)$ for large r (as in Fig. 8), we found that comparison of the two-body approximations to the CW and JF energy expressions provides a very sensitive test of the reliability of our numerical techniques. Ideally, of course, the CW and JF energies should coincide at the two-body level.[6] In practice, evaluation of the CW energy, which involves only integrals $\int d\vec{r}$ over functions that vanish asymptotically at least as fast as r^{-6}, is not plagued by the above finite-box-size effects, in contrast to the situation for the JF form.

The PPA optimization procedure described here and in Sec. II A proves to be quite an efficient algorithm. The most critical of the original four pairs of nonlinear integral equations is eliminated, and replaced by a set of four pairs of linear integral equations (the FHNC′ equations). In general, some ten iterations within the PPA scheme (each iteration involving the calculation of a new correlation function from the current solution of the FHNC and FHNC′ equations) were required to achieve a reasonably accurate solution of the optimization problem, and a few more served to ensure stability. Our optimization procedure is in fact not much more demanding than the determination, within the FHNC framework, of a suitable parametrized choice of $f(r)$, especially if a search in multidimensional parameter space is in the offering. Moreover, the former is clearly preferred in view of the large assortment of further applications of CBF theory, which in any case call for solution of the FHNC′ equations.

The PPA algorithm was found to be workable in a wide density range around the experimental point, the upper density limit depending essentially on the box size chosen. However, it is clear that a reliable study of physical instabilities in both low- and high-density regimes will entail the adoption of substantially refined numerical techniques.[34]

APPENDIX C: MONTE CARLO INTEGRATION TECHNIQUES

The use of Monte Carlo methods makes it possible to evaluate the perturbation correction to the energy without need for further approximations. Moreover, such methods have additional applications in calculating perturbation corrections for other quantities.[24] For present purposes, we consider only the energy correction, which takes the form

$$\frac{\delta\mathcal{E}^{(2,2)}}{A}=-\frac{\nu^2}{2}\left[\frac{3}{4\pi\nu}\right]^3\int d\vec{q}\int d\vec{k}_1\int d\vec{k}_2\, n(\vec{k}_1)[1-n(\vec{k}_1+\vec{q})] \times n(\vec{k}_2)[1-n(\vec{k}_2+\vec{q})]N(\vec{k}_1,\vec{k}_2,\vec{q})/D(\vec{k}_1,\vec{k}_2,\vec{q}) \quad . \tag{C1}$$

where

$$N(\vec{k}_1,\vec{k}_2,\vec{q})=(W_d^2+W_e^2-2\nu^{-1}W_dW_e)/2 \quad , \tag{C2}$$

$$D(\vec{k}_1,\vec{k}_2,\vec{q})=(\epsilon_{\vec{k}_1+\vec{q}}+\epsilon_{\vec{k}_2+\vec{q}}-\epsilon_{\vec{k}_1}-\epsilon_{\vec{k}_2}) \times Z(\vec{k}_1)Z(\vec{k}_2)Z(\vec{k}_1+\vec{q})Z(\vec{k}_2+\vec{q}) \quad ,$$

and

$$W_d=\langle\vec{k}_1+\vec{q},-\vec{k}_2-\vec{q}|\,W(12)\,|\vec{k}_1,-\vec{k}_2\rangle \quad , \tag{C3}$$

$$W_e=\langle\vec{k}_1+\vec{q},-\vec{k}_2-\vec{q}|\,W(12)\,|-\vec{k}_2,\vec{k}_1\rangle \quad .$$

All momentum variables are scaled in units of k_F.

First, the $\vec{q}$ integration is transformed with the identity

$$\int d\vec{q}\,F(q)=\int_0^\infty dq\; w(q)\frac{4\pi q^2F(q)}{w(q)} \quad , \tag{C4}$$

the function $w(q)$ being chosen piecewise linear on the range 0 to Q, where Q is typically 16. For w normalized such that $\int_0^Q dq'\,w(q')=1$, take $\vec{q}=q\hat{q}$, where q solves the quadratic equation

$$u_0=\int_0^q w(q')\,dq' \quad , \tag{C5}$$

in which u_0 is a uniform random number on [0,1]. For this q, the k_1 and k_2 points are drawn independently from the distribution $\theta(1-k)\theta(|\vec{k}+\vec{q}|-1)$. The three components of a $\vec{k}$ are obtained by drawing u_1, u_2, and u_3 independently from the uniform distribution on [0,1]. There are three cases to consider, according to the magnitude of q. We define $c(k,q)=k^2[3k^2+8kq+6(q^2-1)]/24q$ and $f(k)=2k^3/3$. Then, depending on the case, one solves

for b, k, and z in the equations

$$\left.\begin{aligned} &b(q)=c(1,q)-c(1-q,q)\ ,\\ &c(k,q)=b(q)u_1+c(1-q,q)\ ,\\ &z=(1-k^2-q^2)/2kq\ ,\end{aligned}\right\} q<1$$

$$\left.\begin{aligned} &b(q)=c(1,q)-c(q-1,q)+f(q-1)\ ,\\ &u_c=f(q-1)/b(q)\ ,\\ &\left.\begin{aligned} &c(k,q)=b(q)u_1+c(q-1,q)-f(q-1)\ ,\\ &z=(1-k^2-q^2)/2kq\ ,\end{aligned}\right\} u_1>u_c\ ,\\ &\left.\begin{aligned} &f(k)=b(q)u_1\ ,\\ &z=-1\ ,\end{aligned}\right\} u_1<u_c\ ,\end{aligned}\right\} 1<q<2 \qquad \text{(C6)}$$

$$\left.\begin{aligned} &b(q)=\tfrac{2}{3}\ ,\\ &k=u_1^{1/3}\ ,\\ &z=-1\ ,\end{aligned}\right\} 2<q\ .$$

The only operation which cannot be directly carried out is the solution of $c(k,q)=$constant, which is accomplished by Newton-Raphson iteration. Finally, the projection of $\hat{k}$ on the $\hat{q}$ axis is given by

$$\cos(\hat{k}\cdot\hat{q})=(1-z)u_2+z\ , \qquad \text{(C7)}$$

the azimuthal angle of $\hat{k}$ around $\hat{q}$ is

$$k_\phi=2\pi u_3\ , \qquad \text{(C8)}$$

and the weight associated with the volume element $d\vec{k}$ is $2\pi b(q)$.

A single sample of the integral is then given by

$$S=-\tfrac{1}{2}v^2(3/4\pi\nu)^3[4\pi q^2/w(q)][2\pi b(q)]^2N/D\ . \qquad \text{(C9)}$$

The value of the integral is obtained by averaging these samples, while the variance is estimated easily if one also computes the average square of the sample S.

In the first runs, the integrand had not been symmetrized between the direct and exchange terms as displayed in Eq. (C2). This led to a convenient weight $w(q)$ but to occasional positive values of the integrand, although of course the integral itself was correct. When the numerator N was made symmetric, the integrand samples were all negative, but the variance rose because the weight was spread out over a larger range of q. These problems were circumvented by writing

$$N'=N[\theta(q-|\vec{k}_1+\vec{k}_2+\vec{q}|)+\theta(|\vec{k}_1+\vec{k}_2+\vec{q}|-q)]\ . \qquad \text{(C10)}$$

Then, since the integrand is symmetric under the interchange of $\vec{q}$ with $\vec{k}_1+\vec{k}_2+\vec{q}$, one may drop the second Θ function and multiply by an additional factor of 2 to compensate. Thereby the negative definiteness of the integrand is maintained, and, in spite of the extra zeros introduced by the Θ function, a better variance is achieved. Moreover, we note that if the Θ function is zero, the interpolations of the tabulated functions are not necessary.

ACKNOWLEDGMENTS

J.W.C. thanks the Physics Division of Argonne National Laboratory for hospitality and the Argonne Division of Educational Affairs for support while part of this research was done. We enjoyed stimulating discussions relating to various aspects of this work, with the following colleagues: C. E. Campbell, S. Fantoni, A. D. Jackson, M. H. Kalos, L. Lantto, M. A. Lee, M. D. Miller, J. C. Owen, and J. G. Zabolitzky. Some help in the suggestion of using PPA[16] from K. E. Kürten is gratefully acknowledged. This research was supported in part by the Deutsche Forschungsgemeinschaft, the U.S. Department of Energy under Contract No. DE-AC02-76ER13001, and the U.S. National Science Foundation under Grant No. DMR80-08229.

*Present address: Dept. of Physics, Univ. of Illinois, Urbana, Ill. 61801.
†Present address: Dept. of Physics, Texas A & M University, College Station, Tex. 77843.

[1]J. Phys. (Paris) 41, C7 (1980).
[2]J. W. Clark, E. Krotscheck, and R. M. Panoff, J. Phys. (Paris) 41, C7-197 (1980).
[3]W. J. Mullin, Phys. Rev. Lett. 44, 1420 (1980).
[4]L. H. Nosanow, L. J. Parish, and F. J. Pinski, Phys. Rev. B 11, 191 (1975).
[5]J. de Boer, Physica (Utrecht) 14, 139 (1948).
[6]J. W. Clark, in *Progress in Particle and Nuclear Physics,* edited by D. H. Wilkinson (Pergamon, Oxford, 1979), Vol. 2.
[7]D. Schiff and L. Verlet, Phys. Rev. 160, 208 (1967).
[8]V. R. Pandharipande and H. A. Bethe, Phys. Rev. C 7, 1312 (1973).
[9]J. W. Clark, L. R. Mead, E. Krotscheck, K. E. Kürten, and M. L. Ristig, Nucl. Phys. A328, 45 (1979).
[10]K. E. Schmidt and V. R. Pandharipande, Phys. Rev. B 19, 2504 (1979).
[11]D. Levesque, Phys. Rev. B 21, 5159 (1980).
[12]E. Feenberg, *Theory of Quantum Fluids* (Academic, New York, 1969).
[13]J. C. Owen, Phys. Lett. 89B, 303 (1980); Phys. Rev. B 23, 2169 (1981).
[14]E. Krotscheck, Phys. Rev. A 15, 397 (1977); E. Krotscheck and W. Kundt, Phys. Lett. 71B, 19 (1977).
[15]L. J. Lantto and P. J. Siemens, Phys. Lett. 68B, 308 (1977); Nucl. Phys. A317, 55 (1979); L. J. Lantto (private communication).
[16]C. E. Campbell and E. Feenberg, Phys. Rev. 188, 396 (1969); C. C. Cheng and C. E. Campbell, Phys. Rev. B 15, 1438 (1977).
[17]E. Krotscheck, Nucl. Phys. A317, 149 (1979).
[18]E. Krotscheck and M. L. Ristig, Nucl. Phys. A242, 389 (1975); E. Krotscheck, Phys. Lett. 54A, 123 (1975).
[19]E. Krotscheck and J. W. Clark, Nucl. Phys. A328, 73 (1979).
[20]E. Krotscheck and J. W. Clark, Nucl. Phys. A333, 77 (1980).
[21]J. J. MacKenzie, Phys. Rev. 179, 1002 (1969).
[22]J. W. Clark, P. M. Lam, and W. J. Ter Louw, Nucl. Phys. A255, 1 (1975).
[23]E. Krotscheck and R. A. Smith, Phys. Lett. 100B, 1 (1981).
[24]E. Krotscheck, R. A. Smith, and J. W. Clark, in Recent Progress in Many-Body Theories, Springer Lecture Notes in Physics, Vol. 142 edited by J. G. Zabolitzky, M. de Llano, M. Fortes, and J. W. Clark, (Springer, Berlin, to be published), p. 270.
[25]C. W. Woo, Phys. Rev. 151, 138 (1966).
[26]E. Krotscheck, H. Kümmel, and J. G. Zabolitzky, Phys. Rev. A 22, 1243 (1980); E. Krotscheck and J. W. Clark, in *The Many Body Problem, Jastrow Correlations versus Brueckner Theory,* Springer Lecture Notes in Physics, Vol. 138, edited by R. Guardiola and J. Ros (Springer, Berlin, 1980), p. 356.
[27]P. A. Whitlock, D. Ceperley, G. V. Chester, and M. H. Kalos, Phys. Rev. B 19, 5598 (1979).
[28]B. M. Axilrod and E. Teller, J. Chem. Phys. 11, 293 (1943).
[29]D. Levesque and C. Lhuillier, J. Phys. (Paris) 41, C7-191 (1980); C. Lhuillier and D. Levesque, Phys. Rev. B 23, 2203 (1981).
[30]**M. H. Kalos and M. A. Lee (private communication); M. H. Kalos, in Recent Progress in Many-Body Theories, see Ref. 24, p. 252.**
[31]K. E. Kürten and C. E. Campbell, in *The Many Body Problem, Jastrow Correlations versus Brueckner Theory,* see Ref. 26, p. 332.
[32]W. Kolos and L. Wolniewicz, J. Chem. Phys. 43, 2429 (1965); Chem. Phys. Lett. 24, 457 (1974).
[33]M. D. Miller and L. H. Nosanow, Phys. Rev. B 15, 4376 (1977).
[34]L. Castillejo, A. D. Jackson, B. K. Jennings, and R. A. Smith, Phys. Rev. B 20, 3631 (1979); A. D. Jackson, B. K. Jennings, R. A. Smith, and A. Lande, *ibid.* (in press).